Journal of Controlled Release 352 (2022) 163–178

Contents lists available at ScienceDirect

Journal of Controlled Release

journal homepage: www.elsevier.com/locate/jconrel

Physical and barrier changes in gastrointestinal mucus induced by the permeation enhancer sodium 8-[(2-hydroxybenzoyl)amino] octanoate (SNAC)

J.S. Mortensen [a], S.S.-R. Bohr [a,b], S. Harloff-Helleberg [a,c], N.S. Hatzakis [b,d], L. Saaby [e,f], H. M. Nielsen [a,*]

[a] Center for Biopharmaceuticals and Biobarriers in Drug Delivery, Department of Pharmacy, Faculty of Health and Medical Sciences, University of Copenhagen, Universitetsparken 2, DK-2100 Copenhagen, Denmark
[b] Department of Chemistry, Nano-Science Center, Faculty of Science, University of Copenhagen, Bülowsvej 17, DK-1870 Frederiksberg, Denmark
[c] LEO Foundation Center for Cutaneous Drug Delivery, Department of Pharmacy, Faculty of Health and Medical Sciences, University of Copenhagen, Universitetsparken 2, DK-2100 Copenhagen, Denmark
[d] Novo Nordisk Center for Protein Research, Faculty of Health and Medical Sciences, University of Copenhagen, Blegdamsvej 3B, DK-2200 Copenhagen, Denmark
[e] CNS Drug Delivery and Barrier Modelling, Department of Pharmacy, Faculty of Health and Medical Sciences, University of Copenhagen, Universitetsparken 2, DK-2100 Copenhagen, Denmark
[f] Bioneer A/S, Kogle Alle 2, DK-2970 Hørsholm, Denmark

ARTICLE INFO

Keywords:
Permeation enhancer
Salcaprozate sodium
Ex vivo porcine intestinal mucus
Ex vivo porcine gastric mucus
Permeability
Mucus retention force
Rheology
Single particle tracking

ABSTRACT

Drug delivery systems (DDS) for oral delivery of peptide drugs contain excipients that facilitate and enhance absorption. However, little knowledge exists on how DDS excipients such as permeation enhancers interact with the gastrointestinal mucus barrier. This study aimed to investigate interactions of the permeation enhancer sodium 8-[(2-hydroxybenzoyl)amino]octanoate (SNAC) with *ex vivo* porcine intestinal mucus (PIM), *ex vivo* porcine gastric mucus (PGM), as well as with *in vitro* biosimilar mucus (BM) by profiling their physical and barrier properties upon exposure to SNAC. Bulk mucus permeability studies using the peptides cyclosporine A and vancomycin, ovalbumin as a model protein, as well as fluorescein-isothiocyanate dextrans (FDs) of different molecular weights and different surface charges were conducted in parallel to mucus retention force studies using a texture analyzer, rheological studies, cryo-scanning electron microscopy (cryo-SEM), and single particle tracking of fluorescence-labelled nanoparticles to investigate the effects of the SNAC-mucus interaction. The exposure of SNAC to PIM increased the mucus retention force, storage modulus, viscosity, increased nanoparticle confinement within PIM as well as decreased the permeation of cyclosporine A and ovalbumin through PIM. Surprisingly, the viscosity of PGM and the permeation of cyclosporine A and ovalbumin through PGM was unaffected by the presence of SNAC, thus the effect of SNAC depended on the regional site that mucus was collected from. In the absence of SNAC, the permeation of different molecular weight and differently charged FDs through PIM was comparable to that through BM. However, while bulk permeation of neither of the FDs through PIM was affected by SNAC, the presence of SNAC decreased the permeation of FD4 and increased the permeation of FD150 kDa through BM. Additionally, and in contrast to observations in PIM, nanoparticle confinement within BM remained unaffected by the presence of SNAC. In conclusion, the present study showed that SNAC altered the physical and barrier properties of PIM, but not of PGM. The effects of SNAC in PIM were not observed in the BM *in vitro* model. Altogether, the study highlights the need for further understanding how permeation enhancers influence the mucus barrier and illustrates that the selected mucus model for such studies should be chosen with care.

* Corresponding author.
E-mail address: hanne.morck@sund.ku.dk (H.M. Nielsen).

https://doi.org/10.1016/j.jconrel.2022.09.034
Received 10 May 2022; Received in revised form 9 September 2022; Accepted 15 September 2022
Available online 19 October 2022

1. Introduction

In recent years, the interest in oral delivery of macromolecules such as peptides and proteins has increased due to their high specificity, potency and low systemic toxicity. However, due to structural features of such macromolecules, designing drug delivery systems (DDS) adequate for efficient delivery of therapeutic doses after oral administration is challenging [1]. A particular challenge is the poor permeation across the gastrointestinal (GI) epithelium, and in addition, the mucus lining the GI-tract also acts as a selective barrier that limits diffusion of especially macromolecules and particulate DDS [2,3].

The inclusion of functional excipients such as permeation enhancers is currently one of the most successful approaches to improve the absorption of peptides by the oral route [4]. Several potential oral permeation enhancers have been reported in literature [1,4]. However, currently only two permeation enhancers have been approved for use in oral peptide formulations [4]. Oral capsules containing the peptide octreotide and sodium octanoate (C8) in an oily suspension (Mycapssa®, Chiasma, Needham, MA, USA) and tablets containing the semaglutide, a GLP-1 analogue, together with sodium 8-[(2-hydroxybenzoyl)amino] octanoate (SNAC) (Rybelsus®, Novo Nordisk, Bagsværd, Denmark) were approved by the FDA in 2020 and 2019, respectively [5,6]. C8 is a medium-chain fatty acid and SNAC a derivative that also contains both the acid group and a fully saturated C8 chain modified with a hydroxybenzoyl group at the terminus [7]. In contrast to Mycapssa®, which is used for intestinal delivery, Rybelsus® is applied for gastric delivery [1,8]. However, formulations with SNAC intended for intestinal delivery has also shown promising outcomes [7]. Oral absorption of unfractionated heparin as well as cyanocobalamin was reported to be enhanced in the presence of SNAC [7,9]. This led to the approval of cyanocobalamin combined with SNAC in a medical food tablet for vitamin B_{12}-deficient anaemic persons [7,10]. The heparin/SNAC combination tested in a phase III trial (PROTECT) failed to demonstrate superior efficacy compared to enoxaparin treatment as well as suffered from compliance issues due to bad taste [7,11].

Mucus is one of the body's first line of defences in the GI-tract, as it lubricates and protects the underlying epithelium from entry of pathogens and toxic compounds. Mucus is generally comprised of approximately 90–95% (*w*/w) water, 1–5% (*w/v*) mucins, 1–2% (w/w) lipids and small amounts of proteins, DNA, electrolytes, cells and cell debris. However, the specific composition of mucus depends on the regional site of origin, the specie and stimuli from the microenvironment influenced by the overall health condition [2,3,12–14]. The high molecular weight glycoproteins, mucins, comes in different isoforms dependent on the regional site and are considered the structural backbone of the mucus. Mucins entangle into a heterogeneous porous structure, thus are responsible for the size-filtering barrier and the viscoelastic properties of mucus. Additionally, mucins are characterised by being rich in repeated domains of proline, threonine and serine (PTS-domains), which are separated by hydrophobic and cysteine-rich domains. The PTS-domains are densely O-glycosylated with hydrophilic sialic acids and terminal sulphated residues, which provide the mucins with a net negative charge at physiological pH. The hydrophobic and hydrophilic regions in mucins together with their overall negative charge, give mucus its unique physical and interactive barrier properties [2,3,15,16]. These barrier properties of mucus can influence the absorption of macromolecular drugs and the delivery efficacy of DDS when administered to a mucosal surface [2,3]. However, as ionic strength, pH and non-mucin components within mucus can affect the intermolecular mucin interactions, and thus the viscoelastic and barrier properties of mucus [2,14,17–20], excipients may influence the barrier function of mucus. Hence, a better understanding of how excipients such as permeation enhancers interact with the mucus barrier is essential to improve research on oral delivery of macromolecular drugs.

To date, only a few studies have focused on the interaction between permeation enhancers and mucus or assessed if a possible interaction alters either the permeation enhancer functionality or the mucus barrier properties [21,22]. SNAC is a promising permeation enhancer that is reported to increase the overall absorption of semaglutide across the gastric mucosa by buffering the microenvironment to a pH value of approximately 7, which inactivates pepsin and thereby limits the enzymatic degradation of semaglutide [7,8,23]. However, a change in pH can affect intermolecular mucin interactions, and SNAC may therefore also alter the barrier properties of mucus. An increase in pH is generally associated with a reduction in the viscosity of mucus, which based on the Stokes-Einstein relation would correlate with an increased diffusion rate through mucus [13,24–27]. However, Twarog et al., found that the addition of 10–100 mM SNAC increased the viscoelastic modulus G' and G" as well as the viscosity of *ex vivo* porcine intestinal mucus (PIM) [21]. Moreover, they also found that the G' of PIM was increased when exposed to the known mucolytic *N*-acetylcysteine that otherwise is known to decrease G' and viscosity of respiratory mucus [21,28,29]. Overall, more information regarding the effect of SNAC on intestinal mucus and mucus collected from other regional sites are needed.

To develop efficient new DDS for oral delivery of macromolecules, it is important to understand to which extent the mucus is a barrier for delivery in the absence and presence of excipients *e.g.* permeation enhancers. Previous studies have shown that the permeation of molecules through native mucus such as PIM was reduced with increasing molecular weight and cationic charge due to physical hindrance imposed by the mucus mesh and electrostatic interactions within the mucus [3,18]. Yet, the potential effects of permeation enhancers, and their interactions with the intestinal mucus barrier is largely unexplored. As the access to healthy human intestinal mucus is limited, mucus from animals is the best alternative. The general consensus is that PIM shows good resemblance to human intestinal mucus, due to its high structural and viscoelastic similarities [13,30,31]. However, large biological variation can still limit the outcomes from studies with *ex vivo* mucus [18,32]. Therefore, as an alternative to PIM, our group established a *in vitro* biosimilar mucus (BM) model comprised of commercially available compounds [19]. The BM was previously reported to exhibit microstructure and viscoelastic properties similar to PIM [18,19]. However, to which extent the BM reflects the barrier properties of PIM in terms of permeation of charged and neutral macromolecules, and especially how excipient interactions influence the barrier properties of BM has not yet been reported.

In the present study, we hypothesized that SNAC would decrease the viscosity in mucus and hereby cause increased diffusion of macromolecules and nanoparticles across and within mucus, respectively. The aim was therefore to gain information on how SNAC affects the diffusion of macromolecules and nanoparticles in *ex vivo* PIM using several experimental settings and techniques; bulk mucus permeability of a range of charged and neutral macromolecules, retention force and rheology as well as microscale single particle tracking of 250 nm particles and cryo-scanning electron microscopy, and to compare selected effects with parallel studies in *ex vivo* PGM and *in vitro* BM. Overall, this would improve the understanding of SNAC effects on the physical and barrier properties of mucus.

2. Materials and methods

2.1. Materials

Mucin from porcine stomach type II (PGMII), bovine serum albumin (BSA) (>98%), cholesterol (>99%), polysorbate 80 (Tween® 80), neutral fluorescein-isothiocyanate dextrans of 4 (FD4), 10 (FD10), 20 (FD20), 40 (FD40), 59–77 (FD70) and 150 (FD150) kDa, negatively charged fluorescein-isothiocyanate-carboxymethyl dextrans of 4 (FCM4), 40 (FCM40) and 150 (FCM150) kDa, positively charged fluorescein-isothiocyanate-diethylaminoethyl dextrans of 3–5 (FDD4), 40 (FDD40) and 150 (FDD150) kDa, $MgSO_4{\cdot}2H_2O$, $CaCl_2{\cdot}7H_2O$ and

Hank's Balanced Salt Solution (HBSS) were purchased from Sigma-Aldrich (Søborg, Denmark). MES anhydrous BioChemica (MES) was obtained from PanReac AppliChem (Darmstadt, Germany). NaCl and 5 M NaOH were acquired from VWR (Søborg, Denmark) and CHEM-SOLUTE (Roskilde, Denmark), respectively. Cyclosporine A [MEbMT-b-^{3}H] (20 Ci/mmol) and ovalbumin [methyl-^{14}C] (40.0 mCi/mg) were obtained from American Radiolabeled Chemicals Inc. (Saint-Louis, MO, USA). Vancomycin [ring-^{3}H] (11.7 Ci/mmol) was purchased from ViTrax Radiochemicals (Placentia, CA, USA). SPHERO™ fluorescent Nile red polystyrene particles with a diameter of 0.1–0.3 μm (250NPs) were obtained from Nordic BioSite Aps (Copenhagen, Denmark). Polyacrylic acid (PAA) (Carbopol 974P NF, 34,900 mPaS at 0.5% (*w/v*)) and phosphatidylcholine (PC) (>98%) were purchased from Lubrizol (Brussels, Belgium) and Lipoid (Ludwigshafen, Germany), respectively. Sodium 8-[(2-hydroxybenzoyl)amino]octanoate (salcaprozate sodium, >99%) (SNAC) was synthesized by EzBiolab (Shanghai, China).

2.2. Collection of ex vivo porcine intestinal mucus (PIM) and gastric mucus (PGM)

Porcine intestines and stomachs were obtained from healthy gilts used for surgical practice (40–68 kg, approx. 3–4 months of age, Danish Landrace). The pigs were fasted for 18–24 h prior to surgery. Immediately after euthanization, the stomach was removed and up to 8 m of jejunum was isolated distal from the ligament of Treitz. The stomach was cut so the entire epithelial surface could be visualized. The intestine was then cut into 50 cm sections and opened by a longitudinal cut. Due to large amount of food debris, stomachs were rinsed with tap water while no rinsing of the intestines was needed as no or little food debris was found in the intestine. Mucus was gently scraped off the epithelial surface, pooled, aliquoted and stored at −20 °C until analysis. Stomachs, intestines and mucus were kept on ice during isolation to limit possible degradation. PIM and PGM were isolated from different animals. Stomach and intestines were handled according to the authorization for the use of animal by-products and derived products for research and diagnosis approved by the Danish Veterinary and Food Administration (license number DK-13-oth-931833).

2.3. Preparation of in vitro biosimilar mucus (BM)

Preparation of BM was done according to Birch et al. 2018 [33]. Briefly, the BM was prepared by mixing a lipid solution and a mucin solution. The lipid solution was prepared by mixing 3.6% (*w/v*) cholesterol, 18% (w/v) PC, 1.6% (w/v) polysorbate 80 in isotonic buffer (10 mM MES with 1.3 mM $CaCl_2$, 1.0 mM $MgSO_4$ and 137 mM NaCl, pH 6.5) under magnetic stirring. For the mucin solution, PAA was dissolved in 10 mM MES containing 1.3 mM $CaCl_2$, and 1.0 mM $MgSO_4$ (pH 6.5) and then mucin was added under intense magnetic stirring. NaOH was added to the solution to increase pH to around 6 prior to the addition of BSA and the lipid solution. The final BM contained 0.9% (*w/v*) PAA, 5% (w/v) mucin, 100 mM NaOH and 3.1% (w/v) BSA (final concentration of 0.36% (w/v) cholesterol, 0.18% (w/v) PC, 0.16% (w/v) polysorbate 80). The final BM was pH adjusted to 6.5 with minimal amounts of NaOH and stored overnight at 4 °C before use.

2.4. Bulk mucus permeation of peptides, protein and FDs with different charge and molecular weight

Permeation studies through mucus was performed using filter inserts (with tissue culture treated polycarbonate membrane, 1.12 cm^2 for FD studies and 0.33 cm^2 for peptide and protein studies, 0.4 μm pore size) (Corning, Costar Transwell®, Thermo Fisher Scientific, Roskilde, Denmark) and a procedure slightly modified from previously described [33]. To achieve complete coverage of PIM and PGM in the filter inserts to be used in the permeability study, sufficient fluidity was ensured by hydration of PIM and PGM. Specifically, 3.5 parts of PIM or PGM were mixed with 1 part of 10 mM MES in HBSS pH 6.5 (mHBSS) (*v*/v) one day before the experiment and stored at 4 °C.

At the day of the experiment, 250 μL hydrated PIM or 250 μL BM were applied on the 1.12 cm^2 filter inserts and 75 μL hydrated PIM or hydrated PGM were added to the 0.33 cm^2 filter inserts. The filter inserts were allowed to equilibrate for 10 min on a shaking table (37 °C, 50 rpm, Thermo MaxQ 2000, Thermo Fisher Scientific). 1000 μL or 600 μL mHBSS were added to all receiver compartments of the 1.12 cm^2 and 0.33 cm^2 filter inserts, respectively, and the equilibration continued for another 10 min. At 0 min, 100 μL of donor solution consisting of 125 μg/mL FD4, FD10, FD20, FD40, or FD70, 250 μg/mL FD150, FDD4, FDD40, FCM4, or FCM40, 1000 μg/mL FDD150 or FCM150 in mHBSS was gently added dropwise to the donor compartment of the 1.12 cm^2 filter inserts, whereas 30 μL of a 1.0 μCi/mL ^{3}H-cyclosporine A, 1.0 μCi/mL ^{3}H-vancomycin or 0.5 μCi/mL ^{14}C-ovalbumin solution was added to the 0.33 cm^2 filter inserts. At 10–30 min intervals and up to 4 h, samples of 200 μL or 100 μL were collected from the receiver compartments of the 1.12 cm^2 and 0.33 cm^2 filter inserts, respectively. After every sampling, the receiver compartments were replenished with 200 μL or 100 μL mHBSS (37 °C).

The sample fluorescence was quantified at λ_{EX} 485 nm and λ_{EM} 520 nm using 96-well black microplates in a plate reader (FLUOstar Omega, BMG LABTECH, Ortenberg, Germany). For each experiment, new standard curves were prepared by serial dilution in the range of 0.03–2.00 μg/mL (FD10, FD20, FD40, FD70, FD150, FDD40), 0.06–4.00 μg/mL (FD4, FCM40) or 0.13–48.00 μg/mL (FDD4, FDD150, FCM4, FCM150). Acceptable standard curves consisted of minimum four data points with calculated fluorescence intensity deviations of maximum ±15% (± 20% for the lower limit of quantification (LLOQ)) from the measured fluorescence intensity.

For determination of the permeated ^{3}H-cyclosporine A, ^{3}H-vancomycin and ^{14}C-ovalbumin, receiver samples were transferred to scintillation vials with 2 mL scintillation fluid (Ultima Gold, Perkin Elmer, Boston, MA, USA). The samples were measured using a Tri-Carb 2910 TR Scintillation analyzer (Perkin Elmer). Limit of quantification was 10× the background (mHBSS) value.

The steady state flux (J_{SS}, μg/(min · cm^2) or μmol/(min · cm^2)) was calculated as the slope of minimum three data points from the linear section of the accumulated amount (Q, mol/cm^2) of the Q *vs* time (t) plot. Data for the steady state flux was only accepted if the accumulated amount Q to the time point was at sink condition. The apparent permeability coefficient (P_{APP}) was then calculated using Eq. (1), which is a simplified version of Fick's first law with the assumption that $C_{donor} >> C_{receiver}$. Where $C_{0,\ donor}$ is the initial donor concentration.

$$P_{APP} = \frac{J_{SS}}{C_{0,donor}} \quad (1)$$

The lag time was calculated as the linear regression slope's intercept with the x-axis of the Q *vs* time plot. The permeated amount (%) was calculated based on the accumulated amount in the receiver compartment after 240 min relative to the initial amount of added FD, FDD, FCM, peptide or protein.

2.5. Mucus retention force using a texture analyzer

To determine to which extent SNAC affected mucus, the retention forces of mucus were measured using a TA.XT plus texture analyzer (Stable Micro Systems, Godalming, UK) equipped with a 5 kg loading cell. The experiments were conducted using hydrated mucus (*i.e.* 2.5 part mucus to 1 part donor solution) in the filter inserts after the 4 h bulk permeability studies. Before measurement, the filter inserts with mucus were allowed to equilibrate to room temperature for at least 30 min. They were then mounted and retained using a table vice on the texture analyzer, and a cylindrical 10 mm diameter probe was lowered into the mucus at 2 mm/s and kept a 1 mm above the filter membrane for 5 s before the probe was retracted at 10 mm/s. The probe was washed

between each measurement. The force required to retract the probe as a function of probe retraction distance was recorded using the Exponent software (Stable Micro Systems, Godalming, UK). Baseline correction was conducted by subtraction of the average force measured when the retracted probe was no longer in the mucus layer (−6 to −9 mm), as force data and baseline would vary due to different degrees of adhesion to the probe after each measurement. Mucus retention force was defined as the peak force needed to retract the probe from the mucus layer.

2.6. Particle diffusion within mucus using single particle tracking (SPT)

To evaluate how SNAC affected mucus at the microscale level, SPT was employed. 2.5 parts PIM or BM were either vortexed with 1 part mHBSS or SNAC suspended in mHBSS and incubated at 37 °C for 1 h prior the addition of 250NPs. The final concentrations were 150 mM SNAC and 0.08 mg/mL 250NPs in hydrated mucus. Recording were performed without single particle imaging buffer containing oxygen scavengers and triplet state quenchers [34,35] to avoid variations of mucus properties. Samples of 30 μL mucus was carefully added to a microscopy glass slide placed in a custom build Teflon microscopy chamber. Time series was acquired at 37°C by an inverted spinning disk confocal microscope (Olympus SpinSR10, Olympus, Tokyo, Japan) using a 60× oil immersion objective with a 1.4 numerical aperture (Olympus) and a CMOS camera (PRIME 95B, Teledyne Photometrics, Tucson, AZ, USA) yielding final pixel dimensions of 0.183 × 0.183 μm. For each biological sample, a total of 5–10 time series was recorded using the build-in automates stage control to avoid bias from subjectively picking areas to measure. Each measurement was recorded at 166.66 Hz using 532 nm laser excitation for 1000 frames after which the stage would move 300 μm in the x and y directions and continue recording.

For analysis of SPT data, spot detection and trajectory linking was performed using our previously published software [36–39]. For each biological replicate, all 5 to 10 measurements were pooled and subsequent analysis performed on the compiled data. To avoid ensemble averaging, the underlying diffusion coefficient, extracted from each individual trajectory using unbinned maximum likelihood fitting to all trajectory displacements was conducted, as previously demonstrated [40,41]. The probability to observe a given displacement is given by Eq. (2):

$$p(r,t,D) = \frac{r}{2Dt} * e^{\frac{r^2}{4Dt}} \quad (2)$$

where r is the observed displacement, t is the time between consecutive images (6 ms) and D is the diffusion coefficient. Using the Stokes-Einstein relation, the diffusion coefficient could subsequently be converted to viscosity [22].

To examine the degree of particle arrest within mucus, we analyzed particle confinement using mean square displacement (MSD, μm^2) analysis given by Eq. (3):

$$MSD = 4Dt^a \quad (3)$$

Where D is the instantaneous diffusion coefficient, t is the time lag and a is the anomalous diffusion parameter (alpha) describing particle confinement. Finding the alpha value for each observed particle provides an estimate of both immobile ($a < 0.001$), confined ($0.001 < a < 0.5$) and freely moving particles ($0.5 < a$), respectively [42]. Additionally, the apparent trajectory spread within the mucus barrier was evaluated. This was achieved by arbitrarily setting all particle locations to start at the same position and subsequently evaluate their distance to the starting position, thus displaying the average particle coverage. This offers both a qualitative assessment through comparison of 2D coverage plots while also providing quantitative comparisons through the distance of the 98th quantile for all measurements.

2.7. Mucus microstructure visualized by cryo-scanning electron microscopy (cryo-SEM)

For cryo-SEM, 2.5 parts PIM or BM in 1 part mHBSS alone or in presence of SNAC (150 mM final concentration in hydrated mucus) was incubated for 1 h. Thereafter, the sample was sandwiched between two 100 μm cavity planchettes and cryopreserved in liquid N_2. The sandwiched planchettes were mounted in a planchette holder (Leica, Vienna, Austria) under liquid N_2 and transferred to a cryo transfer shuttle (VCT100, Leica). The samples were cracked, sublimated for 4 min at −90°C, and sputter coated (MED020, Leica) with carbon/platinum to a thickness of 6 nm. Samples were examined with a FEI Quanta 3D scanning electron microscope operated at an accelerating voltage of 2 kV with a cryostage temperature of −140°C.

2.8. Alteration in mucus viscoelastic properties by rheological measurements

The rheological measurements of PIM and PGM alone and in the presence of 150 mM SNAC were conducted with an AR-G2 rheometer equipped with a 40 mm truncated cone with a cone angle of 1° and a Peltier plate (TA Instruments, New Castle, DE, USA). Similar to SPT and cryo-SEM, 2.5 parts PIM or PGM in 1 part mHBSS alone or in the presence of SNAC was incubated for 1 h, before 500 uL sample was applied to the plate and covered with solvent trap (TA Instruments) to prevent sample dehydration. The plate temperature was kept at 37°C throughout the measurement. A pre-shear of 100 s^{-1} was applied for 10 s to properly distribute the sample followed by 5 min equilibration. Measurements were conducted in three consecutive steps: 1) a frequency sweep in the range of 0.1–10 rad/s using an oscillation stress of 0.1 Pa ensuring that measurements were conducted within the linear viscoelastic range (LVE), 2) continuous flow ramp step; increasing shear rate of 0.001–3000 s^{-1} over a 30 min period, 3) stress sweep; constant frequency of 1 rad/s, oscillation range of 0.01–500 Pa. Equilibration of 5 min was used between each step allowing the sample to equilibrate.

For investigation of ionic strength and pH dependency of PIM, PIM was hydrated as described above. However, the osmolality of the mHBSS was adjusted by addition of 156 mM NaCl to resemble to the osmolality change of PIM induced by the presence of 150 mM SNAC. Additionally, to mimic the pH induced by 150 mM SNAC, the pH of samples was adjusted by addition of 5 M NaOH.

The relationship between storage and loss modulus (G'/G") at low deformation within the LVE range was used to provide information about the strength of the intermolecular interactions that exist within the mucus network [43]. Comparison of viscosities were conducted at a biologically relevant shear rate of 0.4 s^{-1} [44]. Shear rate dependency was investigated by creating a linear fit to log(viscosity) as a function of log(shear rate) in the range of 0.1–1000 s^{-1}. All r^2 values were minimum 0.95. LVE end was determined by a maximum 5% decline of G' from the mean of the 5 data point of G' within the linear area of the stress sweep. G' < G" transition was determinate as the first oscillation stress values where G'/G" was below 1 in the stress sweep.

2.9. Statistics

All data are presented as means with standard deviations (SD). A student *t*-test or one-way analysis of variance (ANOVA) followed by a Durnett's comparisons test was used to determine if a significant difference was present between two means or three or more means, respectively. In case of unequal variance, a Welch test were used. GraphPad Prism 8.3 for Windows, from GraphPad Software Inc. (La Jolla, CA, USA) was used for all statistical calculations. *P*-values below 0.05 were considered statistically significant. Replicate of different pigs or BM batches are indicated by n, while the number of technical replicates is indicated by N.

3. Results

3.1. SNAC affected bulk permeability and retention force of PIM and BM differently

In vitro permeability experiments were performed to assess whether SNAC at increasing concentrations affected bulk mucus permeation of the macromolecule drug marker FD4 and the pathogen marker FD150 through PIM as well as retention force of PIM. Additionally, it was investigated how the SNAC-mucus interaction was reflected in the BM model. Fig. 1A-F summarizes the calculated permeability coeffcicients (P_{APP}), lag times and the relative permeated amount (%) of FD4 and FD150 through PIM at increasing concentrations of SNAC (0–150 mM).

It was observed that the P_{APP} values and the permeated amount (%) of FD4 (Fig. 1A and G) and FD150 (Fig. 1B and H) through PIM remained unchanged despite the increasing SNAC concentrations. However, the lag time for permeation across the PIM decreased with increasing SNAC concentration, especially for FD150 (Fig. 1E) and to a lesser extent for FD4 (Fig. 1D). Even though the lag times decreased ($p < 0.0001$) with up to 50% for FD150 through PIM in the presence of 150 mM SNAC, the

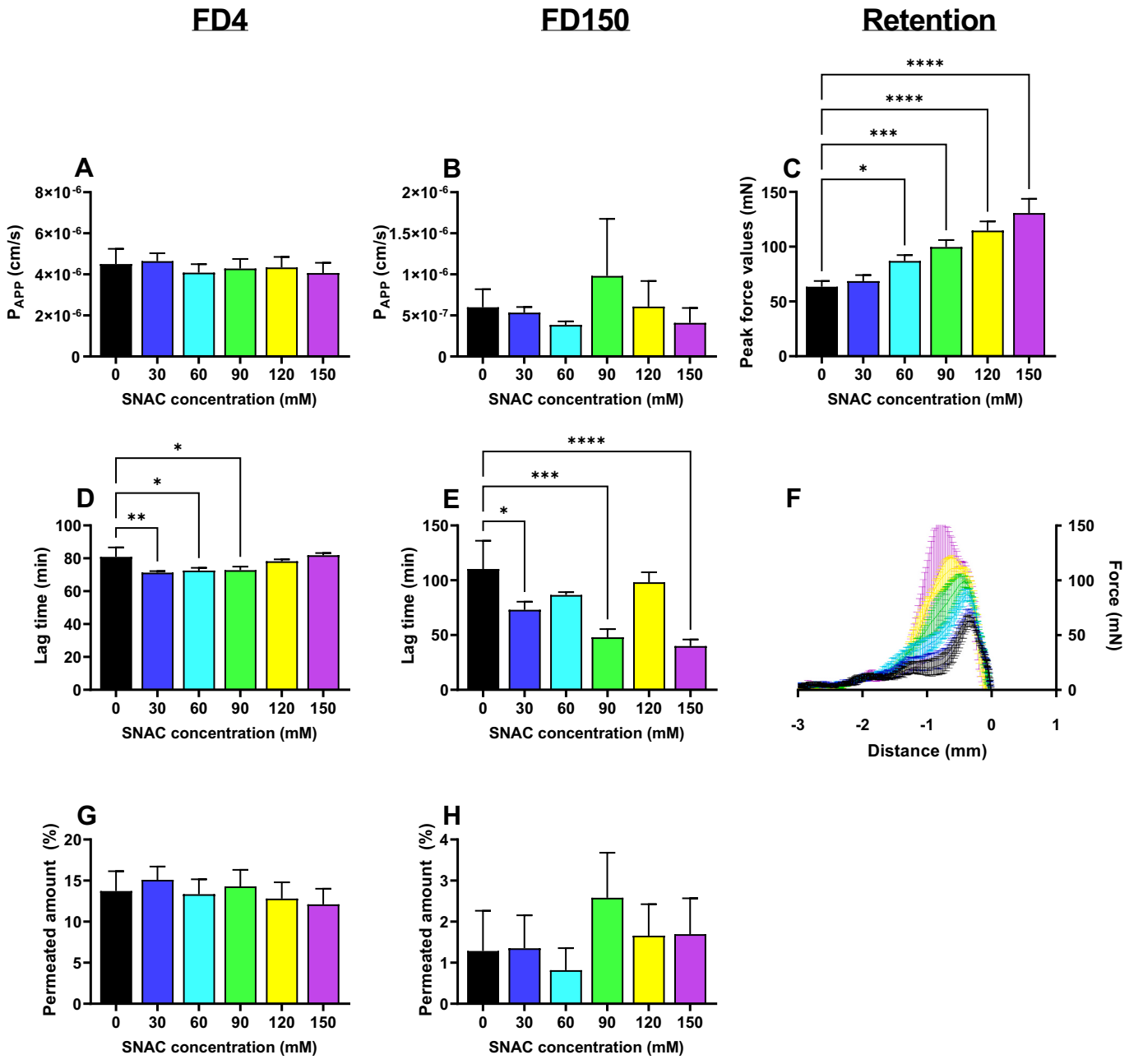

Fig. 1. A, B) Apparent permeability coefficients (P_{APP}), D, E) lag times and G, H) permeated amounts (%) after 240 min of adding fluorescein-isothiocyanate dextrans (FDs) of 4 kDa and 150 kDa at different sodium 8-[(2-hydroxybenzoyl)amino]octanoate (SNAC) concentrations (0–150 mM) through *ex vivo* porcine intestinal mucus (PIM). C) Retention force (*i.e.* peak values of retraction force) and F) force of retraction as a function of the probe retraction distance from PIM after 4 h exposure to different SNAC concentrations; 0 mM (black), 30 mM (blue), 60 mM (turquoise), 90 mM (green), 120 mM (yellow), and 150 mM (purple). Data are given as means of biological replicates with standard deviations, $n = 2–3$, $N = 2$. In two cases, P_{APP} values for FD150 kDa were below the quantification limit and omitted, thus resulting in a low n for some FD150 data. Data are statistically different from the 0 mM SNAC condition as stated by * ($p < 0.05$), ** ($p < 0.01$), *** ($p < 0.001$) or **** ($p < 0.0001$). (For interpretation of the references to colour in this figure legend, the reader is referred to the web version of this article.)

total amount permeated remained similar, probably due to a slight decrease in the P_{APP}-value.

To investigate if the addition of SNAC altered the mucus retention force (*e.g.* force needed to retract a submerged probe from the PIM layer), this was measured using the filter insert with PIM exposed to 0–150 mM SNAC from the permeability study. The peak force of retention values (maximal forces recorded) and full retention force diagrams are shown in Fig. 1C and F, respectively. SNAC concentrations

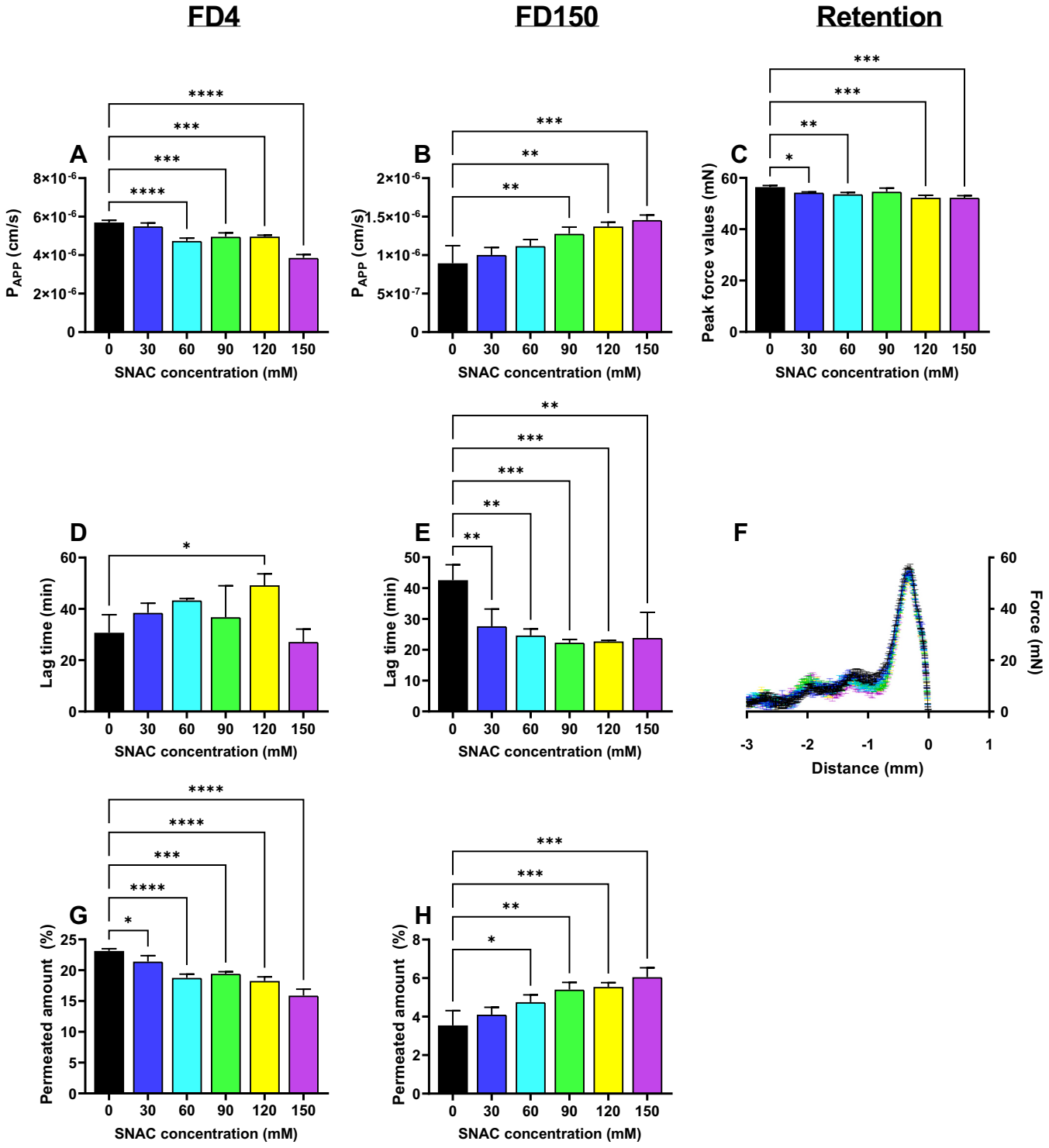

Fig. 2. A, B) Apparent permeability coefficients (P_{APP}), D, E) lag times and G, H) permeated amounts (%) after 240 min of adding fluorescein-isothiocyanate dextrans (FDs) of 4 kDa and 150 kDa at different sodium 8-[(2-hydroxybenzoyl)amino]octanoate (SNAC) concentrations (0–150 mM) through biosimilar mucus (BM). C) Retention force (*i.e.* peak values of retraction force) and F) force of retraction as a function of the probe retraction distance from BM after 4 h exposure to different SNAC concentrations; 0 mM (black), 30 mM (blue), 60 mM (turquoise), 90 mM (green), 120 mM (yellow), and 150 mM (purple). Data are given as means with standard deviations, $n = 3$, $N = 2$. Data are statistically different from the 0 mM SNAC condition as stated by * ($p < 0.05$), ** ($p < 0.01$), *** ($p < 0.001$) or **** ($p < 0.0001$). (For interpretation of the references to colour in this figure legend, the reader is referred to the web version of this article.)

between 60 and 150 mM increased the retention forces in a concentration-dependent manner and the measured peak retention force in the presence of 150 mM SNAC was increased ($p < 0.0001$) by >100% compared to the control without SNAC (Fig. 1C). Additionally, increased SNAC concentrations increased the elasticity of PIM, as the force peaks shifted towards longer probe retraction distances (*i.e.* the probe was retracted longer before detaching from the mucus) (Fig. 1F).

It was further investigated if the BM model could reflect the interaction with SNAC as observed in PIM. Fig. 2 summarizes the permeation data for FD4 and FD150 through BM in the presence of different SNAC concentrations (0–150 mM).

The P_{APP} values and the permeated amounts of FD4 in BM decreased with increasing SNAC concentrations, whereas the lag times were independent of SNAC concentrations except for samples exposed to 120 mM SNAC (Fig. 2A, D and G). Interestingly, the effect of SNAC on the permeation of the pathogen marker, FD150, through BM was opposite compared to effects of SNAC observed for permeation of FD4. The P_{APP} values and permeated amount for FD150 were increased ($p < 0.01$) in the presence of 90, 120 and 150 mM SNAC, while the lag time for FD150 decreased ($p < 0.01$) 1.6–1.9-fold when BM was exposed to SNAC (Fig. 2B, E and H). The retention force of BM decreased slightly with increasing concentrations of SNAC (Fig. 2C) however, the elasticity of BM was unaffected by the presence of SNAC, as the force peaks did not shift towards longer probe retraction distances (Fig. 2F).

Overall, the effect of SNAC on the BM permeability and retention force were in contrast to the observed effect of SNAC on PIM as bulk permeation of FD4 and FD150 through PIM was found unaffected by the presence of SNAC, while the retention force increased concentration-dependently (Fig. 1C). A concentration of minimum 60 mM SNAC was generally needed to induce changes ($p < 0.05$) in the permeability of BM

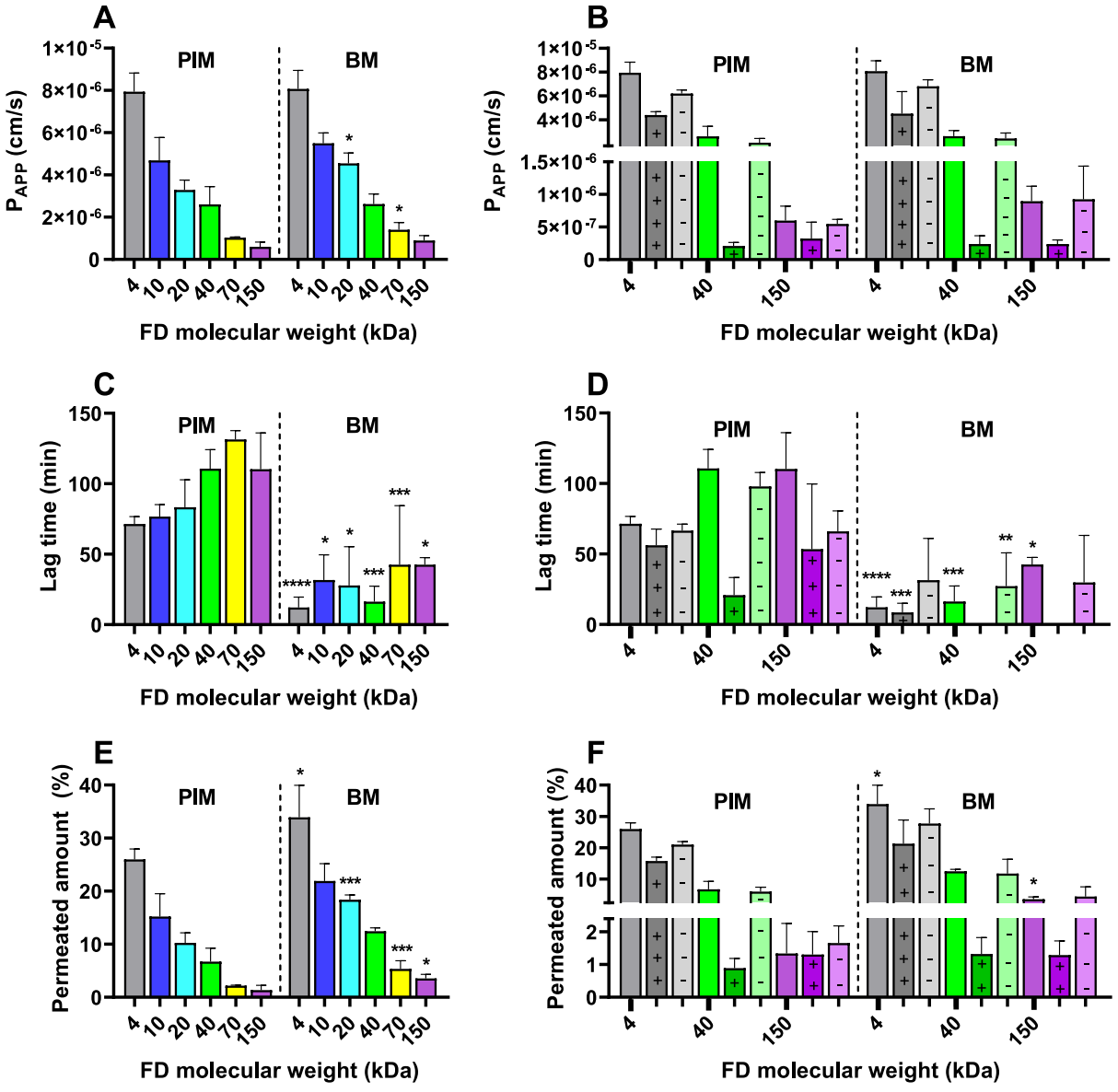

Fig. 3. A, B) Apparent permeability coefficients (P_{APP}), C, D) lag times and E, F) permeated amounts (%) after 240 min of initially added fluorescein-isothiocyanate dextrans (FDs) of 4 (grey), 10 (blue), 20 (turquoise), 40 (green), 70 (yellow), and 150 (purple) kDa through *ex vivo* porcine intestinal mucus (PIM) or biosimilar mucus (BM). A, C, E) Neutral FDs with different molecular weight, B, D, F) neutral (empty bar), positively (plus) and negatively (minus) charged FDs of different molecular weights. Data are given as means with standard deviations, $n = 2–9$, $N = 1–3$. In one case, data was below the limit of quantification for positively charged FD 40 kDa, thus the n is low for positively FD40 kDa. Comparison of values between the individual FDs through PIM and BM are statistically different as stated by * ($p < 0.05$), ** ($p < 0.01$), *** ($p < 0.001$) or **** ($p < 0.0001$). (For interpretation of the references to colour in this figure legend, the reader is referred to the web version of this article.)

and the retention force of PIM and BM. However, the use of 150 mM SNAC induced the largest effect in all cases.

3.2. Bulk permeation of different molecular weight and charged FDs through PIM and BM was similar

As observed in Figs. 1 and 2, the presence of SNAC affected the permeability of PIM and BM differently. To investigate if this difference was due to PIM and BM having different size filtering and charge interactive barrier properties, macromolecular permeation of FDs with different molecular weight and charge through PIM and BM was determined. Fig. 3 summarizes calculated P_{APP} values, lag times and permeated amounts (%) of FDs of different molecular weights (4–150 kDa) and with different charges (neutral; FD, positive; FDD, and negative; FCM) from bulk permeability experiments through PIM and BM.

As shown in Fig. 3A, P_{APP} values decreased similarly with increasing molecular weight of the neutral FDs in both PIM and BM, and only the P_{APP} values for FD20 and FD70 were different ($p < 0.05$) in the two models. Likewise, the P_{APP} values of negatively and positively charged FDs in PIM and BM were found to be similar. In general, positively charged FDs showed a decreased permeation compared to that of neutral and negatively charged FDs (Fig. 3B). This effect depended on the FD molecular weight, as P_{APP} values of positively charged 4 and 150 kDa FDs were reduced 2-fold, while P_{APP} of 40 kDa was reduced 11–12-fold

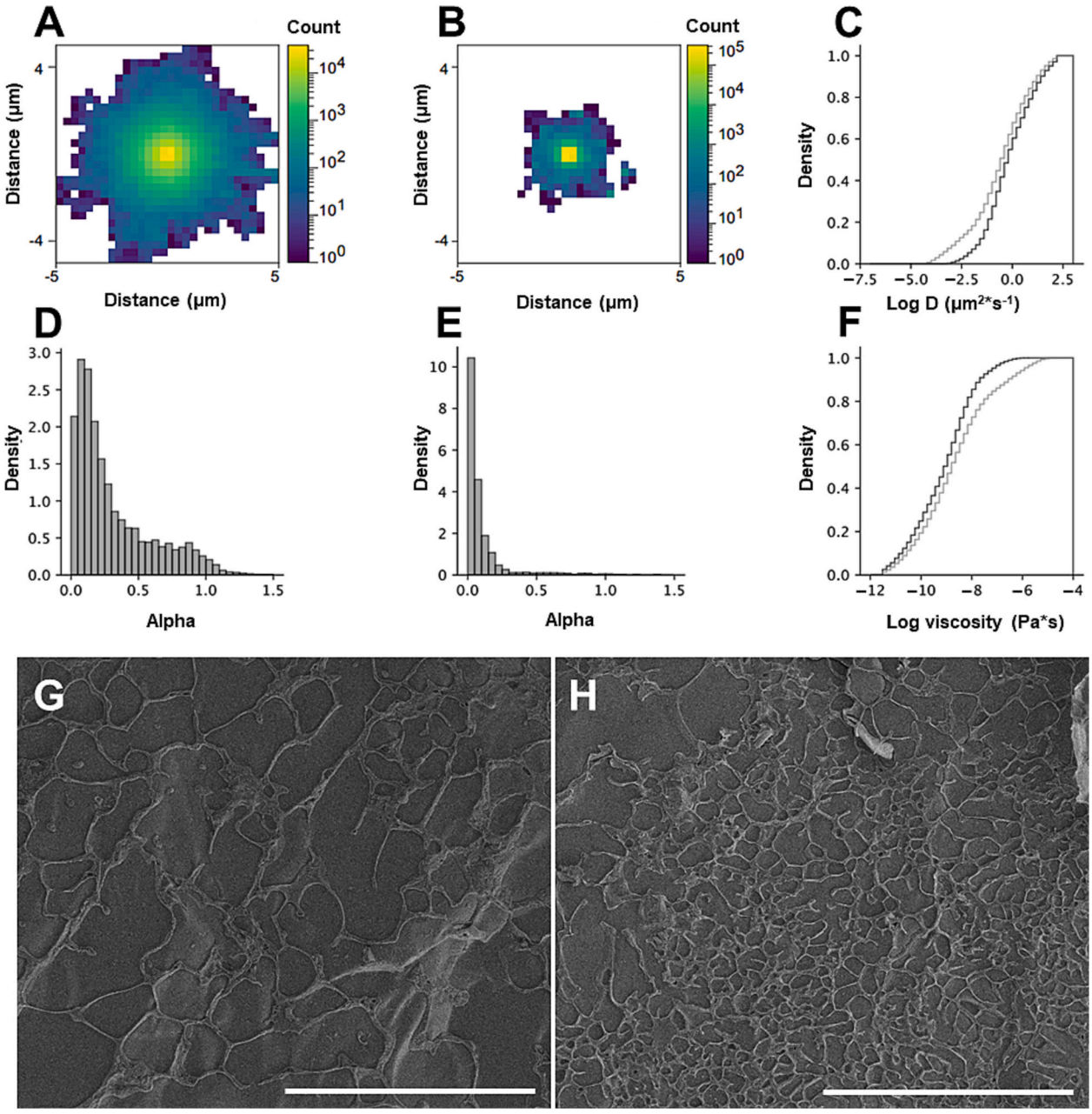

Fig. 4. A, B) 2D heatmaps of average particle coverage and D, E) bar plots of alpha values calculated from individual particles *vs* the densities of 250 nm Nile red polystyrene particles (250NPs) in *ex vivo* porcine intestinal mucus (PIM) in the absence (A, D) (10,347 particles) and presence (B, E) of 150 mM sodium 8-[(2-hydroxybenzoyl)amino]octanoate (SNAC) (7310 particles), respectively. C) Cumulative diffusion coefficients and F) cumulative viscosities of 250NPs in PIM in the absence (black) and presence (grey) of 150 mM SNAC. G, H) Representative cryo-scanning electron microscopy (cryo-SEM) images of PIM in the absence (G) or presence (H) of 150 mM SNAC. Cryo-SEM scale bar represent 20 µm. Data in A-F are given as the mean of 3 biological replicates ($n = 3$). (For interpretation of the references to colour in this figure legend, the reader is referred to the web version of this article.)

compared to that of the neutral FDs in both PIM and BM. Lagtimes in PIM increased with molecular weight, neutral and negative charges of the FD, whereas no clear trend in lagtimes for permeation through the BM was observed. Overall, the lag times observed in BM were significantly decreased compared those observed in PIM, except for the positively charged FD40 and FD150 as well as negatively charged FD4 and FD150 (Fig. 3C and D). The permeated amounts of neutral 4, 20, 70 and 150 kDa FDs through BM were higher compared to that through PIM (Fig. 3E), whereas most permeated amounts of negatively and positively charged FDs through BM were similar to that through PIM (Fig. 3F). However, overall PIM and BM displayed similar size filtering and interactive barrier properties as permeation was similar for a large range molecular weight and charged FDs.

3.3. *Effect of SNAC on particle diffusion in and microstructure of PIM and BM*

To further investigate the effects of SNAC on mucus barrier properties on a microscopic level, SPT was used to study the particulate movement of 100–300 nm polystyrene particles *i.e.* 250NPs in PIM and BM in the absence or presence of 150 mM SNAC. For visualization of the microstructural alteration induced by SNAC in mucus, cryo-SEM was employed.

The average particle coverage of the diffusion of numerous particles

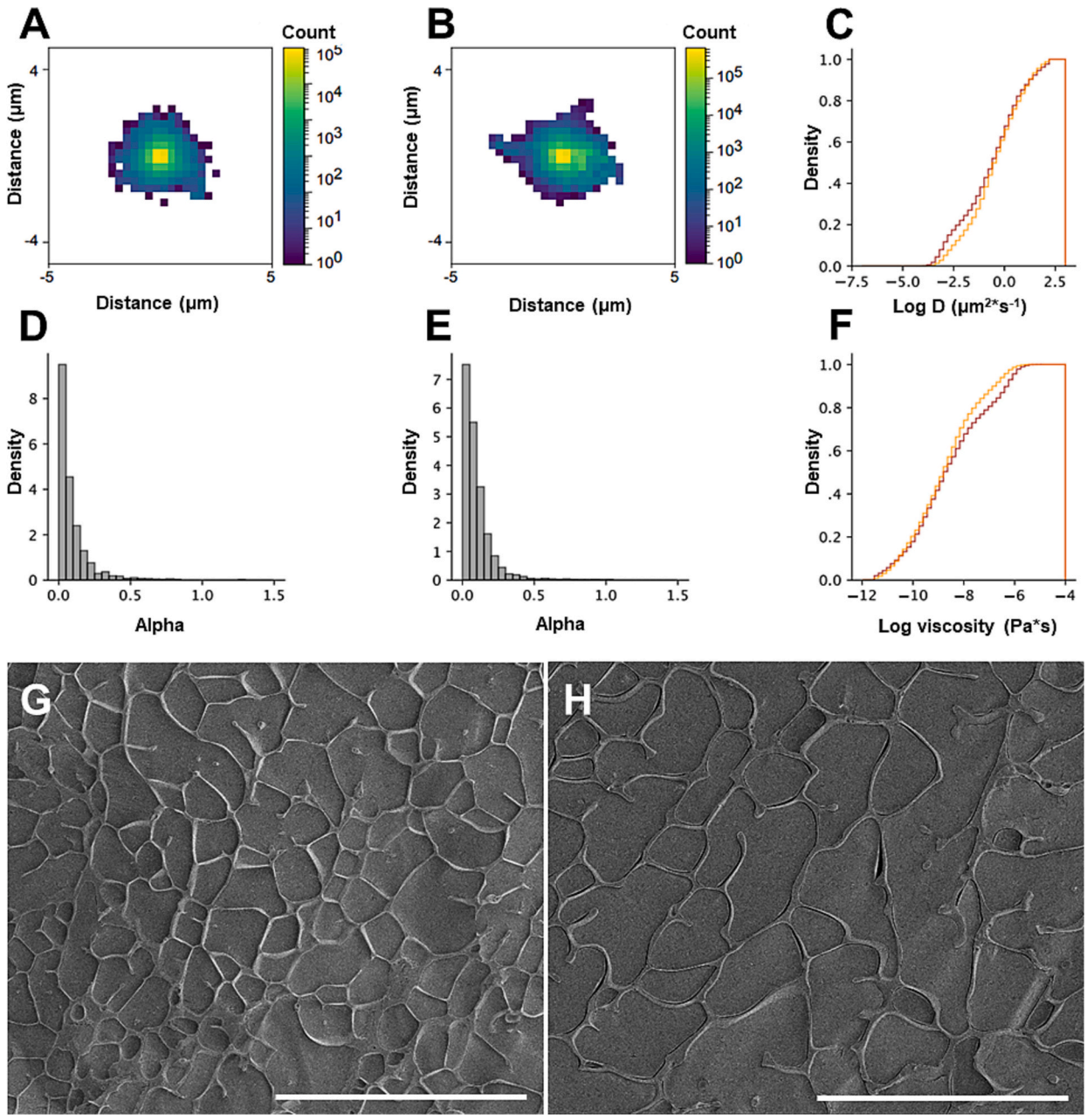

Fig. 5. A, B) 2D heatmaps of average particle coverage and D, E) bar plots of alpha values calculated from individual particles *vs* the densities of 250 nm Nile red polystyrene particles (250NPs) in biosimilar mucus (BM) in the absence (A, D) (7572 particles) and presence (B, E) of 150 mM sodium 8-[(2-hydroxybenzoyl)amino] octanoate (SNAC) (9841 particles), respectively. C) Cumulative diffusion coefficients and F) cumulative viscosities of 250NPs in BM in the absence (red) and presence (yellow) of 150 mM SNAC. G, H) Representative cryo-scanning electron microscopy (cryo-SEM) images of BM in the absence (G) or presence (H) of 150 mM SNAC. Cryo-SEM scale bar represent 20 μm. Data in A-F are given as the mean of $n = 3$. (For interpretation of the references to colour in this figure legend, the reader is referred to the web version of this article.)

were calculated and visualized in average particle coverage plots in Fig. 4A and B. Additionally, from each particle trajectory, the diffusion coefficient (D) was calculated and with Stokes-Einstein relationship converted into the viscosity (termed microviscosity). To elucidate the reason for altered particle diffusion, MSDs were calculated from observed particle displacements and fitted to extract the anomalous diffusion parameter, alpha, describing particle confinement similarly to previously published [42]. Results of studies in PIM are summarized in Fig. 4.

Evaluation of average particle coverage in PIM (Fig. 4A and B) revealed a significant ($p < 0.001$) decrease in the area of particle motion from 3.35 ± 0.47 μm^2 to 0.42 ± 0.03 μm^2 in the presence of 150 mM SNAC, indicating that SNAC causes obstruction of diffusion of particles in PIM. Diminished particle diffusibility was further indicated by comparing the diffusion coefficients of all recorded trajectories. Here we observed lower diffusion through PIM in the presence of 150 mM SNAC (Fig. 4C), displayed by a left-shift of the distribution. To confirm particle confinement as indicated in Fig. 4A and B, the distribution of alpha values was compared. Here particle confinement increased as indicated by a decrease in alpha values in mucus exposed to SNAC (Fig. 4E) when compared to the control (Fig. 4D), in excellent agreement with the earlier observations of particle coverage and diffusion. As expected, little free Brownian motion (alpha = 1) was observed in PIM. Thresholds on the alpha values were set based on particle confinement in buffer (Supplementary information Fig. S1, and Methods Section 2.6). The immobile particle fraction changed ($p < 0.001$) from 20.5 ± 7.3% to 67.2 ± 3.1%, the confined fraction ($p < 0.01$) from 61.9 ± 6.5% to 31.4 ± 2.5% and the freely moving fraction from 17.7 ± 8.3% to 1.4 ± 0.9% in the absence and presence of 150 mM SNAC, respectively. Thus, the immobile fraction of particles increased >3-fold in the presence of SNAC and barely any particles in the freely moving fraction were detected. At the same time, the microviscosity also shifted towards higher viscosities in the presence of SNAC (Fig. 4F). The high particle confinement and low diffusion could be explained by a much tighter network within PIM induced by the presence of 150 mM SNAC. By visual inspection of the cryo-SEM images, it is observed that SNAC considerably, but somewhat heterogeneously, decreased the pore size of PIM (Fig. 4G) compared to that of the control (Fig. 4H).

To further understand how SNAC interacts with the BM model at a microscopic scale, and if this might reflect the interaction between SNAC and PIM, SPT and cryo-SEM of BM in the absence and presence of 150 mM SNAC were investigated. Fig. 5 summarizes these data.

The average particle coverage in BM as depicted in the coverage plots (Fig. 5A and B) did not change ($p > 0.05$) in the presence of 150 mM SNAC. Similarly, both cumulative particle diffusion coefficients and microviscosities were primarily unaffected by the presence of 150 mM SNAC (Fig. 5C and F). In contrast, the particle confinement slightly decreased as seen by increased alpha values in BM in the presence of 150 mM SNAC compared to the control. The immobile particle fraction changed from 63.0 ± 4.4% to 55.4 ± 3.1%, the confined fraction ($p < 0.05$) from 35.9 ± 3.4% to 43.9 ± 3.3% and the freely moving fraction from 1.1 ± 1.1% to 0.7 ± 0.2% in the absence and presence of 150 mM SNAC, respectively (Fig. 5D and E). The slight decrease in particle confinement in the presence of 150 mM SNAC can be explained by the clear disruption of the pore structure within BM in the presence of 150 mM SNAC as visualized by the cryo-SEM images in Fig. 5G and H. Though, compared to the amount of disruption visualized in BM in the presence of 150 mM SNAC, one would expect that the particle confinement would decrease more in the presence of SNAC than observed. Overall, the effect of SNAC on particle diffusion, particle confinement and structure in BM was in contrast to the observed effect of SNAC in PIM as well as the effect on bulk permeability of BM. Even in the absence of SNAC, particle confinement in BM was significantly higher compared to that in PIM as the immobile particle fraction, confined fraction and freely moving fraction were 3, 2 and 18 times higher in BM than PIM, respectively.

3.4. SNAC induced enhanced viscoelastic properties of PIM but not of PGM

To understand the mechanism on how SNAC interacts with the mucus barrier and if this interaction depends on the regional site that mucus was collected from, rheological experiments with PIM and PGM were carried out in the absence and presence of 150 mM SNAC. In these experiments, the effect of 150 mM SNAC on the intermolecular interactions (G' and G'/G" ratio), viscosity, shear dependency (viscosity slope) and stability of the gel network (LVE end and G' < G" transition) were determined to assess how treatment with 150 mM SNAC affected the gel structure of *ex vivo* mucus. Results shown in Fig. 6 represent biological replicates only, as the animal to animal varation were larger than the technical variation on the same sample (Supplementary information Fig. S2).

In the absence of SNAC, both PIM and PGM displayed predominant elastic properties (G' > G"). The G' for PIM increased 64-fold ($p < 0.01$) when exposed to SNAC, indicating the presence of more intermolecular interactions within PIM when exposed to SNAC (Fig. 6B). For PGM, G' also tended to increase in the presence of SNAC, though not statistically significant (Fig. 6B). In the presence of SNAC, the G'/G" ratio for PIM increased ($p > 0.01$) compared to control PIM (Fig. 6C), which indicated that SNAC induced stronger intermolecular interactions in PIM. A similar tendency was observed by the increased G'/G" ratio for PGM exposed to SNAC, though for PGM the effect was not statistically significant due to the relatively large variation between data (Fig. 6C). Comparing the effect of SNAC on PGM samples from individual animals, SNAC induced an increase in G' within each animal (3-, 11- and 36-fold). However, a similar effect on the G'/G" ratio was not observed within PGM compared to that observed in PIM. The G'/G" ratio increased 2- and 6-fold for two animals and was not changed in the third animal in the presence of SNAC. In the absence of SNAC, both PIM and PGM showed shear thinning properties (Fig. 6D). At a shear rate of 0.4 s^{-1}, representing a biologically relevant shear rate [44], the presence of SNAC significantly increased the viscosity of PIM 15-fold ($p < 0.001$). In contrast, SNAC did not change the viscosity of PGM and especially the PGM not exposed to SNAC suffered from high inter-animal variation (Fig. 6E). On the individual animal level, SNAC decreased the viscosity of PGM at 0.4 s^{-1} 4–5 fold in two animals whereas the viscosity was unchanged in the other animals. In the absence of SNAC, shear rate dependency was higher ($p < 0.01$) for PGM than for PIM, and the presence of SNAC increased the shear rate dependency of PIM (Fig. 6F). Thus, in the presence of SNAC, the gel network within PIM was less stable towards higher shear rates. Stability of PIM towards stress induced deformation (LVE end and G' < G" transition) was slightly increased in the presence of SNAC, though not statistically significant due to a relatively high variation between animals (Fig. 6G and I). For PGM, no effect on the LVE was observed in the presence of SNAC, though the G' < G" transition tended to decreased in the presence of SNAC (Fig. 6I).

In the presence of 150 mM SNAC, the pH of PIM increased from 6.44 ± 0.07 to 7.25 ± 0.21 and for PGM it increased from 6.36 ± 0.90 to 7.31 ± 0.18. Additionally, the ionic strength of PIM and PGM also increased in the presence of 150 mM SNAC, as the osmolality increased from 404 ± 18 to 614 ± 100 mOsM, and from 234 ± 10 to 446 ± 10 mOsM, respectively. With these results in mind, it was investigated whether the previously mentioned increased G', G'/G" ratio and viscosity of PIM in the presence of 150 mM SNAC could be explained by changes in pH and osmolality. Indeed, increasing the ionic strength and pH of PIM with NaCl and NaOH to mimic the changes induced by exposing PIM to 150 mM SNAC changed the viscoelastic properties of PIM, though not to the same extent as with 150 mM SNAC (Supplementary information Fig. S3). Only the G'/G" ratio and G' < G" transitions were not significantly different from those observed in the 150 mM SNAC sample.

Overall, the effects of SNAC were clearly different in the PIM compared those observed in PGM, although the PIM and PGM not

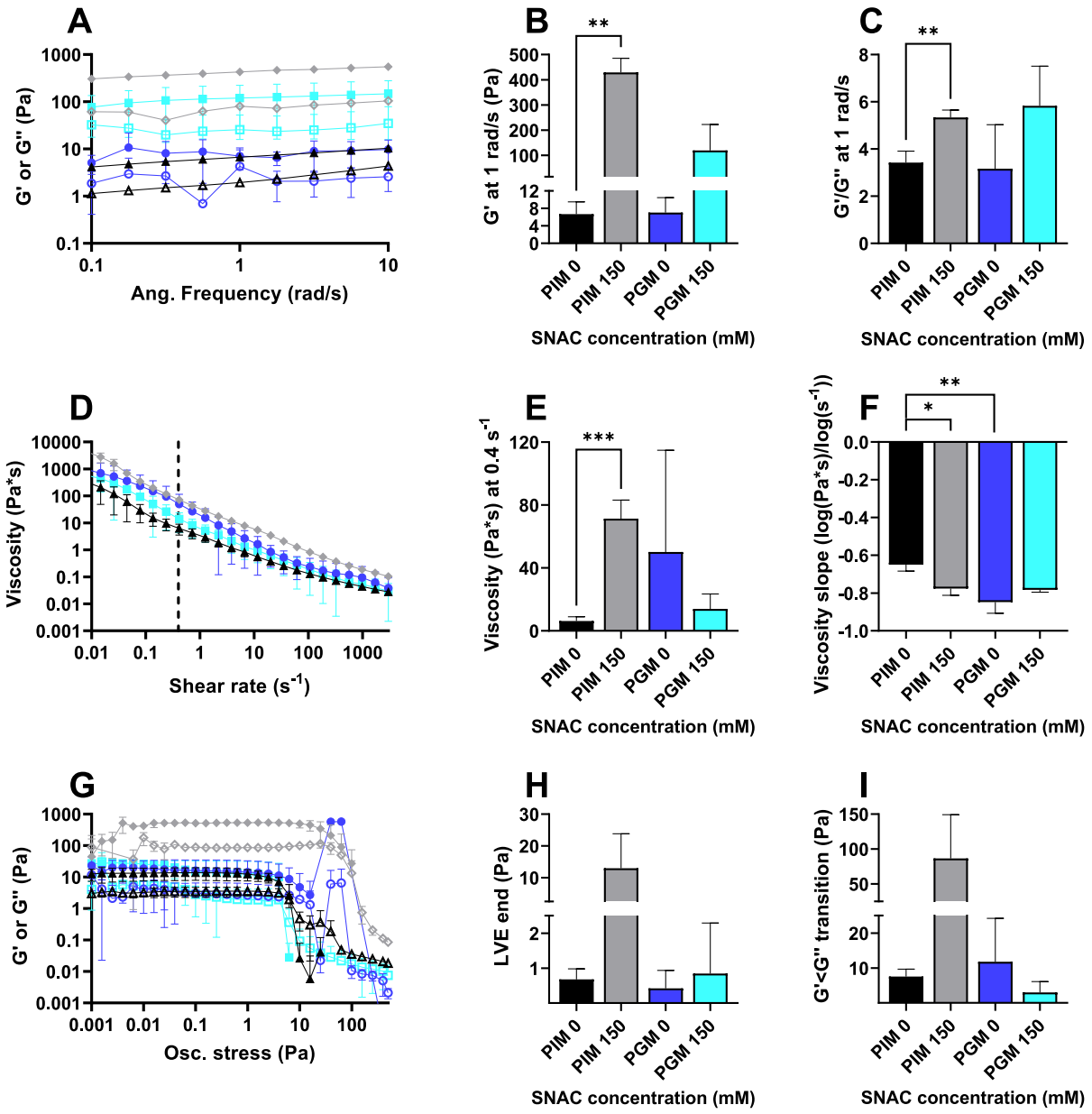

Fig. 6. A) Angular (ang.) frequency sweep with constant oscillation stress of 0.1 Pa, B) storage modulus G' at 1 rad/s, C) storage/loss modulus (G'/G") ratios at 1 rad/s, D) viscosity as a function of shear rate, E) viscosities at 0.4 s^{-1}, F) viscosity slopes of the linear fit between 0.1 and 3000 s^{-1}, G) oscillatory (osc.) stress sweep with 1 rad/s, H) end of linear viscoelastic range (LVE end) and I) G' < G" transition of *ex vivo* porcine intestinal mucus (PIM) and *ex vivo* porcine gastric mucus (PGM) in the absence (PIM: black triangles, PGM: blue circles) and presence of 150 mM sodium 8-[(2-hydroxybenzoyl)amino]octanoate (SNAC) (PIM: grey diamonds, PGM: turquoise squares). G' and G" are indicated by filled and open symbols, respectively. Data are given as means with standard deviation as error bars ($n = 3$–4). Data are statistically different from the 0 mM conditions as indicated by * ($p < 0.05$), ** ($p < 0.01$) or *** ($p < 0.001$). (For interpretation of the references to colour in this figure legend, the reader is referred to the web version of this article.)

exposed to SNAC displayed similar viscoelastic behavior, except for shear rate dependency. Thus, the effect of SNAC on mucus viscoelastic properties depended on the regional site that mucus was collected from.

3.5. SNAC altered bulk permeation through mucus differently depending on mucus source and peptide/protein charge

To establish if the findings by rheology regarding different effects of SNAC on PIM and PGM translate into different barrier properties, we investigated the bulk permeation of two peptides and a protein representing different charge and molecular weights. For these experiments, cyclosporine A (1202 Da), vancomycin (1485 Da) and ovalbumin (44,500 Da) were evaluated as relevant compounds as SNAC is explored for enhancing the absorption of peptides and proteins. At the investigated pH levels in absence of SNAC (*e.g.* 5.0–6.9), cyclosporine A (pI 4.7) and ovalbumin (pI 4.6) will predominantly be net negatively charged, while vancomycin (pI 7.2) will predominantly be net positively charged. However, when 150 mM SNAC is added, a pH buffering will occur and vancomycin is expected to be net neutral [33,45]. The calculated P_{APP}-values and permeated amounts of the different peptides in the absence and presence of 150 mM SNAC are displayed in Fig. 7.

The P_{APP}-value for cyclosporine A through PIM was not affected by

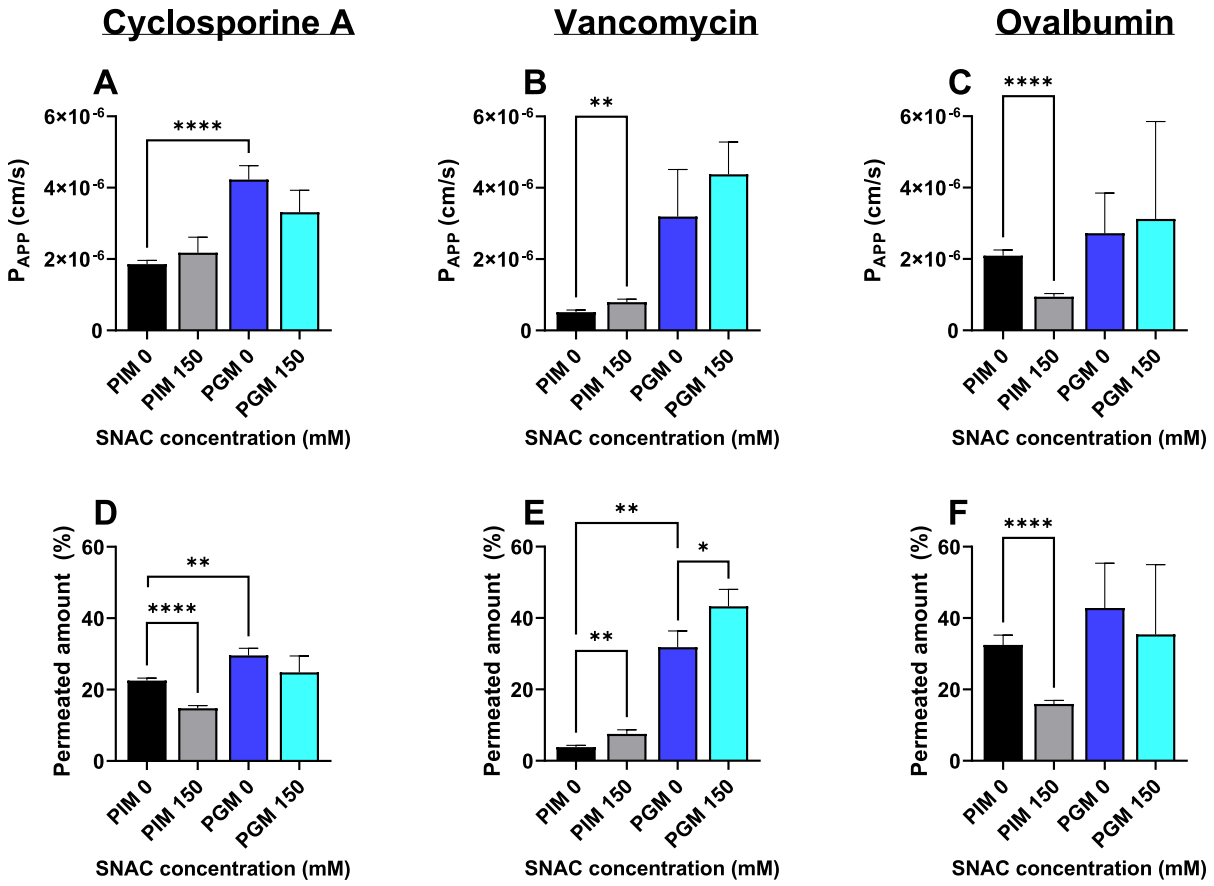

Fig. 7. A, B, C) Apparent permeability coefficients (P_{APP}) and D, E, F) permeated amounts (%) after 240 min of adding cyclosporine A, vancomycin or ovalbumin in the absence (0 mM) and in the presence of 150 mM sodium 8-[(2-hydroxybenzoyl)amino]octanoate (SNAC) through *ex vivo* porcine intestinal mucus (PIM) or *ex vivo* porcine gastric mucus (PGM). Data are given as means with standard deviation as error bars ($n = 3$–4). Data are statistically different from the 0 mM conditions as indicated by * ($p < 0.05$), ** ($p < 0.01$) or **** ($p < 0.0001$).

the presence of 150 mM SNAC (Fig. 7A), whereas the permeated amount of cyclosporine A through PIM decreased approximately 35% ($p < 0.0001$) in the presence of SNAC (Fig. 7D). In contrast, the P_{APP}-value and the permeated amount of cyclosporine A through PGM were not changed significantly in the presence of 150 mM SNAC, although SNAC tended to decrease the permeation of cyclosporine A through PGM ($p > 0.05$). For ovalbumin, 150 mM SNAC decreased ($p < 0.0001$) the P_{APP}-value and permeated amount through PIM by approximately 50%, whereas permeation of ovalbumin through PGM was not affected by SNAC (Fig. 7C and F). Interestingly, the P_{APP}-values and permeated amounts of vancomycin increased ($p < 0.05$) through both PIM and PGM in the presence of 150 mM SNAC by about 50–100% and 40%, respectively (Fig. 7B and E). Permeation of the different compounds through PGM not exposed to SNAC was generally higher (30–625%) than through PIM not exposed to SNAC though this was only found statistically significant for the P_{APP}-value of cyclosporine A (Fig. 7A) and permeated amounts of cyclosporine A and vancomycin (Fig. 7D and E).

Overall, complementing the rheological data displaying that SNAC affected PIM and PGM differently, the presence of 150 mM SNAC altered the permeation of cyclosporine A, vancomycin and ovalbumin through PIM ($p < 0.05$), but not through PGM. The permeated amount of vancomycin through PGM was increased ($p < 0.05$) in the presence of SNAC (Fig. 7E). Hence, the effect of SNAC on the bulk permeation of two peptides and a protein also depended on the regional site that mucus was collected from.

4. Discussion

As more and more DDS for oral delivery of macromolecular drugs *e.g.* peptides include functional excipients such as permeation enhancers to improve mucosal absorption of peptides, it is essential to understand if and how these excipients might modulate the mucus barrier and whether the interaction with the mucus barrier limits the functionality of the excipients.

In the present study, the effect of the permeation enhancer SNAC's interaction with PIM, PGM and BM was investigated utilizing several orthogonal bulk and microscopic techniques. For the first time, we report on the retention force of mucus as an indicator of altered barrier properties of mucus by using a texture analyzer. Retention, *i.e.* measurement of retraction force, is often used to assess the mucoadhesion of a material to a piece of *ex vivo* tissue [46,47]. This novel application of the method enables collection of information on how a treatment can affect mucus properties in the exact same experiment with mucus used for a bulk permeability study.

4.1. Effect and mode of action of SNAC depends on the regional site of mucus collection

It was hypothesized that SNAC would buffer the pH in PIM, which would reorganize the mucin network and disrupt the mucus barrier facilitating increased diffusion though PIM. The addition of SNAC did increase the pH in mucus, however, the presence of 30–150 mM SNAC did not affect the bulk permeation of the hydrophilic drug marker FD4 and the pathogen marker FD150 through PIM. In contrast, the presence

of 150 mM SNAC was found to decrease the bulk permeation of the (at the investigate pH levels) negatively charged cyclosporine A and ovalbumin through PIM, whereas the permeation of the (at investigated pH levels) positively charged vancomycin was increased in the presence of SNAC. Interestingly, the retention force and elasticity of PIM increased when exposed to 60 mM or higher concentrations of SNAC, suggesting that SNAC at those concentrations indeed altered the gel-network of PIM. Complementary to the findings regarding the retention force and the bulk permeation of cyclosporine A and ovalbumin, SPT studies found that the presence of 150 mM SNAC decreased the particle diffusion observed as a higher degree of confinement of the 250 nm polystyrene particles in PIM. The decreased diffusion correlated with increased microviscosity, probably due to the tightened network in the microstructure in PIM observed in the presence of 150 mM SNAC by cryo-SEM. The bulk rheological investigation of PIM also revealed increased G', G'/G" and viscosity of PIM in the presence of 150 mM SNAC, similar to the findings of Twarog et al. [21]. In contrast, the bulk viscoelastic properties of PGM as well as permeation of cyclosporine A and ovalbumin through PGM were overall unaffected by the presence of 150 mM SNAC. Only the permeated amount of vancomycin through PGM was found to be increased in presence 150 mM SNAC, similar to that observed in PIM. Thus, the mode of action of SNAC differed depending on the regional site that mucus was collected from.

According to our hypothesis, the presence of 150 mM SNAC buffered the pH of PIM and PGM to pH 7.3–7.6 independent of the initial pH of PIM or PGM used in these studies (Supplementary information Table S1). Additionally, as SNAC was used in its salt form, the ionic strength of PIM and PGM also increased when exposed to SNAC. The overall behavior and properties of mucus have been shown, in part, to depend on the pH and the ionic strength of mucus [2]. While a pH increase (acidic to neutral) is generally associated with a reduction of the viscosity of mucus [13,24–27], the effect of increased ionic strength in mucus is more debatable. Addition of $CaCl_2$ and NaCl to mucus was previously reported to increase the G' and viscosity as well as the particle confinement in porcine gastric mucin solutions (PGMS) [25] and in *ex vivo* PIM [27,48–50], but also to increase the particle diffusion in and the fluidity of PGMS [13,51,52]. In our study, the addition of 150 mM SNAC significantly increased the rheological properties (*i.e.* G', G'/G' ratio and viscosity) of PIM, but not of PGM. Increasing the pH and ionic strength of PIM with NaOH and NaCl also increased the G' and viscosity of PIM, but not near to the extent as induced by 150 mM SNAC. In contrast, the G'/G" ratio of PIM with increased ionic strength at both pH 6.5 and 7.6 was similar to the G'/G" ratio of PIM with 150 mM SNAC. The G'/G" ratio (*i.e.* ratio between the stored and loss energy after deformation) can relate to information regarding the stability of the intermolecular interactions in a material, as a higher G'/G" ratio suggests strengthened intermolecular interactions, *e.g.* formation of covalent bonds or ionic-dipole interaction bonds rather than weaker hydrogen bonds [43]. As the G'/G" ratio was similar for PIM in the presence of SNAC and at increased ionic strength with NaCl, the stronger intermolecular interactions induced by SNAC were probably predominantly ionic interactions (ionic-dipole) due to the increased ionic strength. Interestingly, as the G' and G'/G" ratio increased for PIM and tended to increase for PGM in the presence of 150 mM SNAC, yet only resulted in a viscosity change of PIM and not of PGM, this suggests that the potentially increased ionic interactions can lead to a reorganization of the mucin network and stabilization of PIM, but not of PGM. A higher degree of post-translational modifications with sialic acids responsible for the negative charge (pKa 2.6) have been identified on MUC2 in the small intestines (*i.e.* PIM) compared to MUC5AC in the stomach (*i.e.* PGM) [53–55], which might explain why PGM is less sensitive towards ionic interactions compared to PIM. Additionally, this higher degree of negative charge in PIM compared to PGM may explain why the permeation of the positive charges peptide vancomycin was less hindered through PGM compared to PIM. Interestingly, Twarog et al., reported an increased G' and viscosity of *ex vivo* PIM in the presence of SNAC, but also in the presence of the known mucolytic *N*-acetylcysteine (NAC) [21]. Normally, NAC is used in treatment of severe lung disorder to reduce pulmonary mucus viscosity and ease exacerbation of mucus [56]. The predominant gel-forming mucin in the lungs are MUC5AC similar to the main mucin subtype found in the stomach [57]. Hence, SNAC/NAC and other excipients- or drug-mucus interactions might indeed depend on the specific mucin and thus the regional site of the mucus barrier.

SNAC being a fatty acid derivative also alters the lipid composition in mucus exposed to SNAC. Yildiz et al. reported that additions of food-associated lipids to *ex vivo* PIM led to a 10–142-fold decrease in the diffusion of 200 nm particles with different surface chemistries [27]. Lipids and especially phospholipids are known to interact with the hydrophobic domains of mucins, stabilizing the extended mucin structure in an aqueous environment [18–20]. To date, most of our understanding on how alteration in *e.g.* ionic strength, pH and the presence of exogenous compounds (*e.g.* lipids) affect the mucus barrier comes from investigation with simplified mucin models, mainly PGMS, though it is well-known that these simplified mucin dispersions do not display similar properties to that of native mucus [31,32,58,59]. Our study adds to a more complete understanding and suggests that there might be regional mucus differences (*e.g.* PGM *vs* PIM) of importance in relation to the effect of ionic strength and exposure to SNAC/fatty acids. Thus, there is a need for further understanding how alteration in physiochemical properties (*e.g.* ionic strength and pH) and composition (fatty acids/lipids) of mucus can affect the native mucus at different regional sites.

4.2. Inter-animal variations in PGM properties may originate from differences in food content

Throughout this study, the data collected using PGM displayed high inter-animal variation compared to that obtained with PIM, irrespective of whether SNAC was present. PGM samples were obtained from two groups of pigs from the same experimental facility, of similar sizes (40–50 kg) and both fasted overnight with access to straw. Despite this, the visual appearances of the PGM samples were very different, with PGM samples from one group being yellow and homogeneous, and PGM samples from the other group being whiter and more clumped (Supplementary information Fig. S5). This also relates to that the stomach contents differed by one group of pigs having mainly yellow digested (fluid-like) food residues and the other group of pigs having solid food residues.

The pH of untreated and hydrated PGM (pH 6.36 ± 0.90) was found similar to that of the corresponding PIM (pH 6.44 ± 0.07), whereas the osmolality of the samples of PGM (234 ± 10 mOsm) was half of what was observed in the corresponding PIM (404 ± 18 mOsm). While these osmolality and pH values of hydrated PIM were found similar to previously reported data on unhydrated PIM (*i.e.* 385–453 mOsm; pH 6.8–7.1 [18,60,61]), the pH of hydrated PGM used in our study was found to be relative high considering the expected low pH environment in the stomach and as previously reported pH of 5.6 [60]. We tested whether the observed pH and osmolality levels of hydrated PGM was explained by the gastric mucosa being extensively rinsed with tap water (pH 7 and 12 mOsm) to remove straw debris prior to PGM collection. However, extensive rinsing with tap water did not affect the pH of the collected PGM, but the osmolality of PGM was somewhat decreased (with 67–101 mOsm) (Supplementary information Table S2). The osmolality of the PGM samples from the two groups of pigs was similar, whereas pH and viscosity varied greatly (Supplementary information Table S1). Difference in food content could likely be the cause of the pH variation between the PGM samples from the two groups of pigs, as gastric acid secretion is upregulated upon food stimuli [62]. Additionally, Henze et al. reported that gastric pH in fasted pigs is highly variable [63], which may also explain the variable pH of the PGM samples observed in this study.

However, even though the PGM samples differed depending on which group of pigs was used, the overall result was consistent: The presence SNAC did not affect the rheological properties and bulk permeability of PGM.

4.3. The BM model reflects the hydrophilic macromolecular drug permeation through PIM, but SNAC interaction effects differ

As low accessibility and high biological variation challenges routine use of intestinal mucus, access to reliable mucus models representing mucus properties is essential. We hypothesized that the BM model would reflect similar macromolecular drug permeation and effect of SNAC as the PIM due to their similar microstructure and viscoelastic properties [18,19].

As mucus is known for both its size filtering and interactive barrier properties [3], this should also be reflected by the BM model. Bulk permeation of FDs through PIM and BM was found to decrease with molecular weight and cationic charge. Important to mention is that the negatively charged membrane material of the filter did not limit the diffusion of the investigated macromolecules. The reduction in P_{APP} values for diffusion of even the positively charged FDDs was not due to the membrane material, as the P_{APP} values for FDs, FDDs and FCMs diffusion through mucus in all cases were at least 20 times lower than through an empty filter (Table S3). Thus, in these settings, the mucus constitutes the main barrier for the permeation of FDs, FDDs and FCMs. Somewhat comparable to our findings, Bhattacharjee et al., found that nanoparticle diffusion through *ex vivo* PIM was reduced with increasing particle size and cationic surface-modifications [64].

In the present work, the BM model was found to have similar size filtering and charge interaction bulk properties as PIM, since the P_{APP}-values obtained in the two models for permeation of FDs with different molecular weights (4–150 kDa) and charge (neutral, negative and positive) through BM were similar. However, the nanoparticle (250 nm) confinement in BM was much higher than in PIM, as the freely moving particle fraction was 17 times more reduced in BM compared to PIM. This is similar to the observation of Huck et al., who reported that the mobility of larger (500 nm) carboxylated polystyrene particles was eight times more reduced in BM than in *ex vivo* PIM [42]. BM was previously reported to hinder the permeation of the hydrophobic molecule testosterone more than for hydrophilic molecules like mannitol and FD4 [18,42], which might explain the poor correlation between particle confinement of hydrophobic polystyrene nanoparticles in BM and PIM compared to bulk permeation of hydrophilic FDs in this study.

Notably, the presence of SNAC was found to decrease the permeation of FD4, but increase the permeation of FD150 through BM, while the retention decreased with increasing SNAC concentrations. SPT and cryo-SEM studies revealed that SNAC did not affect the nanoparticle diffusion in BM, but induced disruption of the BM microstructure. Thus, the BM model did not display interactions with SNAC similar to those with PIM neither at a bulk nor at a microscopic level.

Overall, our results suggest that BM is similar to PIM with regard to bulk permeation of hydrophilic macromolecules such as FDs within a broad molecular weight and charge range. The BM model does, however, not reflect the *ex vivo* situation with regards to interactions with the permeation enhancer SNAC. The BM model is comprised of commercial porcine gastric mucin, lipids, BSA, salts and the viscosity modifier PAA. The use of gastric mucin might explain the difference between BM and PIM in the presence of SNAC, as SNAC affected the viscoelastic properties of PIM and PGM differently. Hence, the BM model may instead more closely resemble PGM than PIM.

4.4. Orthogonal bulk and microscopic techniques improve understandings of SNAC-mucus interactions

Studies on interactions between excipients like permeation enhancers and mucus are to date limited in number and typically reported using only one experimental technique [21,22,33]. This constitutes a risk to limit or overlook important information regarding the mucus interactions. Therefore, we aimed at utilizing several bulk techniques (*i.e.* permeability, retention and rheology) as well as microscopic approaches (*i.e.* SPT and cryo-SEM) to provide better insight into SNAC-mucus interactions. For PIM, the presence of 150 mM SNAC resulted in increased retention, particle confinement, structural network condensation and viscoelastic property changes in terms of increased amounts and strength of intermolecular interaction as well as increased viscosity. Thus, the results obtained with these orthogonal techniques were complementary. However, the bulk permeability study was not conclusive. The addition of 150 mM SNAC did not affect the bulk permeation of the hydrophilic macromolecules FD4 and FD150 through PIM, whereas the bulk permeation through PIM was decreased for the peptide cyclosporine A and the protein ovalbumin, but increased for the peptide vancomycin. While the decreased permeation of cyclosporine A and ovalbumin through PIM in presence of SNAC correlate with the retention, SPT and rheology data, it is interesting that vancomycin permeation increased in presence of SNAC. In the investigated pH range of 6.4–7.3 (*i.e.* pH of hydrated PIM in the absence and presence of 150 mM SNAC), vancomycin will (with an isoelectric point of 7.2 [45]) display a predominant (72–86%) net positive charge at 0 mM SNAC (pH 6.4–6.8), but in presence of 150 mM SNAC (pH 7.3) have a net neutral charge. It is therefore likely, that the increased permeation of vancomycin through PIM and PGM in the presence of 150 mM SNAC is explained by less interaction with the negatively charged mucins, than a direct effect of SNAC on the mucus.

Thus, the reason for the limited permeation enhancing efficiencies of SNAC when considering the FD macromolecules and peptides/protein permeation relative to the significantly higher particle confinement as determined in the SPT studies with PIM in the presence of SNAC may be that an interaction between SNAC and the permeant is necessary for observing an altered permeation/diffusion in PIM. SNAC is reported to enhance the permeation of multiple compounds across intestinal mucosa [21,65], and some drug specificity of SNAC to that end was reported by Buckley et al., who found that SNAC enhanced the absorption of semaglutide, but not of the analogue liraglutide, which is more hydrophobic than semaglutide [8,23]. However, as SNAC alone in this study increased the bulk viscosity of PIM as well as inducing microstructural alterations of PIM, it is more likely that the increased particle confinement was due to the denser microstructural network within PIM with reduced the pore sizes, which limited the peptide permeation and particle diffusion rather than the above speculated effect of SNAC-permeant interaction.

It is interesting, that SNAC increased the viscosity of and particle confinement in PIM as well as decreased permeation through PIM as SNAC has been reported to enhance the permeation of multiple compounds across intestinal mucosa [21,65]. Although that cystic fibrosis mucus displays high viscoelastic properties (*i.e.* G'), which can limit nanoparticle diffusion compared to that in lower viscoelastic mucus, Sanders et al. found nanospheres of 124–560 nm to diffuse easier through high viscoelastic cystic fibrosis sputum compared to low viscoelastic sputum samples [14,66]. The authors hypothesized that their observations were due to the sputum becoming 'more macroporous when the sputum becomes more viscoelastic' [66]. Indeed, this is in line with our findings that although SNAC decreased the average pore size in PIM, the microstructure became more heterogeneous, which may account for our unexpected findings.

Overall, based on our findings, SNAC increased the barrier properties of PIM and the alterations induced by SNAC in PIM and PGM were different. Although direct translation in terms of the importance of these observations to clinical settings needs further studies, the detailed information on SNAC-mucus interactions and the different effects in mucus from different regional sites can improve the understanding of permeation enhancer-mediated oral delivery of macromolecular drugs.

5. Conclusions

To the best of the authors' knowledge, this is the first study investigating the interaction between a functional excipient, specifically the permeation enhancer SNAC, and *ex vivo* PIM and *ex vivo* PGM using an arsenal of both bulk and microscale techniques. While SNAC did not significantly affect bulk permeation of the drug marker FD4 and the pathogen marker FD150 through *ex vivo* PIM, bulk permeation of the peptide, cyclosporine A, and the protein, ovalbumin, through PIM decreased. Additionally the retention force of and particle confinement in *ex vivo* PIM increased in the presence of SNAC. Moreover, SNAC exposure increased the intermolecular ionic interactions within and the viscosity of *ex vivo* PIM as well as induced a denser pore network. Interestingly, the effect of SNAC was found to depend on the regional site that mucus was collected from, as the viscosity and bulk permeation of cyclosporine A and ovalbumin through *ex vivo* PGM was unaffected by exposure to SNAC. Within a range of different molecular weight and differently charged macromolecules, the bulk permeability data obtained with the *in vitro* BM model reflected those obtained with *ex vivo* PIM. However, the effects of SNAC in the two models were different as SNAC seemed to disrupt the BM network with resulting increased bulk permeation of FD150 and larger pore sizes while the particle confinement in BM remained unaffected by the presence of SNAC.

Overall, this study highlights the need for improved understanding on how excipients like permeation enhancers of importance for oral peptide delivery, influence the mucus barrier. It further underlines that the mucus models for such studies should be chosen with care and investigated using a panel of orthogonal techniques.

CRediT authorship contribution statement

J.S. Mortensen: Conceptualization, Methodology, Validation, Formal analysis, Investigation, Data curation, Writing – original draft, Visualization, Project administration. **S.S.-R. Bohr:** Methodology, Software, Validation, Formal analysis, Investigation, Data curation, Writing – original draft. **S. Harloff-Helleberg:** Conceptualization, Methodology, Validation, Writing – review & editing, Supervision. **N.S. Hatzakis:** Validation, Resources, Writing – review & editing, Supervision. **L. Saaby:** Conceptualization, Methodology, Validation, Writing – review & editing, Supervision. **H.M. Nielsen:** Conceptualization, Methodology, Validation, Resources, Writing – review & editing, Supervision, Funding acquisition.

Declaration of Competing Interest

The authors declare no conflicts of interest.

Data availability

Data will be made available on request.

Acknowledgement

The Department of Experimental Medicine (University of Copenhagen, UCPH) are greatly acknowledged for providing pig intestines. Laboratory technician Karina Vissing, scholar student Sylvester Petersen and Master student Lasse Krog (Department of Pharmacy, UCPH) are acknowledged for their help with mucus collection. The Novo Nordisk Foundation is acknowledged for funding the project (Grand Challenge Program NNF16OC0021948 through the Center for Biopharmaceuticals and Biobarriers in Drug Delivery (BioDelivery), UCPH). Additionally, this work was supported by the Lundbeck Foundation (project no. R303-2018-2968). Further, the Innovative Medicines Initiative Joint Undertaking (European Union's Seventh Framework program FP7/2007-2013 and EFPIA: 115363) and the Carlsberg Foundation are acknowledged for support.

Appendix A. Supplementary data

Supplementary data to this article can be found online at https://doi.org/10.1016/j.jconrel.2022.09.034.

References

[1] D.J. Brayden, T.A. Hill, D.P. Fairlie, S. Maher, R.J. Mrsny, Systemic delivery of peptides by the oral route: formulation and medicinal chemistry approaches, Adv. Drug Deliv. Rev. 157 (2020) 2–36.
[2] J. Leal, H.D.C. Smyth, D. Ghosh, Physicochemical properties of mucus and their impact on transmucosal drug delivery, Int. J. Pharm. 532 (1) (2017) 555–572.
[3] M. Garcia-Diaz, D. Birch, F. Wan, H.M. Nielsen, The role of mucus as an invisible cloak to transepithelial drug delivery by nanoparticles, Adv. Drug Deliv. Rev. 124 (2018) 107–124.
[4] S. Maher, D.J. Brayden, Formulation strategies to improve the efficacy of intestinal permeation enhancers, Adv. Drug Deliv. Rev. 177 (2021), 113925.
[5] Anonymous, RYBELSUS® (semaglutide) Tablets for oral use: U.S. Food and Drug Administration [Available from: https://www.accessdata.fda.gov/drugsatfda_docs/label/2019/213051s000lbl.pdf, 2019.
[6] Anonymous, MYCAPSSA® (octreotide) Delayed-Release Capsules for Oral Use: U.S. Food and Drug Administration [Available from, https://www.accessdata.fda.gov/drugsatfda_docs/label/2020/208232s000lbl.pdf, 2020.
[7] C. Twarog, S. Fattah, J. Heade, S. Maher, E. Fattal, et al., Intestinal permeation enhancers for oral delivery of macromolecules: a comparison between salcaprozate sodium (SNAC) and sodium caprate (C10), Pharmaceutics. 11 (2) (2019).
[8] S.T. Buckley, T.A. Baekdal, A. Vegge, S.J. Maarbjerg, C. Pyke, et al., Transcellular stomach absorption of a derivatized glucagon-like peptide-1 receptor agonist, Sci. Transl. Med. 10 (467) (2018).
[9] S.D. Berkowitz, V.J. Marder, G. Kosutic, R.A. Baughman, Oral heparin administration with a novel drug delivery agent (SNAC) in healthy volunteers and patients undergoing elective total hip arthroplasty, J. Thromb. Haemost. 1 (9) (2003) 1914–1919.
[10] M.C. Castelli, D.F. Wong, K. Friedman, M.G. Riley, Pharmacokinetics of oral cyanocobalamin formulated with sodium N-[8-(2-hydroxybenzoyl)amino] caprylate (SNAC): an open-label, randomized, single-dose, parallel-group study in healthy male subjects, Clin. Ther. 33 (7) (2011) 934–945.
[11] A.R. Neves, M. Correia-da-Silva, E. Sousa, M. Pinto, Strategies to overcome Heparins' low oral bioavailability, Pharmaceuticals. 9 (3) (2016) 37.
[12] M. Boegh, H.M. Nielsen, Mucus as a barrier to drug delivery - understanding and mimicking the barrier properties, Basic Clin. Pharmacol. Toxicol. 116 (3) (2015) 179–186.
[13] S.K. Lai, Y.Y. Wang, D. Wirtz, J. Hanes, Micro- and macrorheology of mucus, Adv. Drug Deliv. Rev. 61 (2) (2009) 86–100.
[14] J.S. Mortensen, M.B. Stie, S. Harloff-Helleberg, H.M. Nielsen, Overcoming the mucus barrier, in: L.S. Milane, M.M. Amiji (Eds.), Organelle and Molecular Targeting, 1st ed., CRC Press, Boca Raton, 2021.
[15] J. Dekker, W.M.O. Van Beurden-Lamers, A. Oprins, G.J. Strous, Isolation and structural analysis of rat gastric mucus glycoprotein suggests a homogeneous protein backbone, Biochem. J. 260 (3) (1989) 717–723.
[16] I. Brockhausen, Sulphotransferases acting on mucin-type oligosaccharides, Biochem. Soc. Trans. 31 (2) (2003) 318–325.
[17] L. Thim, F. Madsen, S.S. Poulsen, Effect of trefoil factors on the viscoelastic properties of mucus gels, Eur. J. Clin. Investig. 32 (7) (2002) 519–527.
[18] M. Boegh, S.G. Baldursdottir, A. Mullertz, H.M. Nielsen, Property profiling of biosimilar mucus in a novel mucus-containing in vitro model for assessment of intestinal drug absorption, Eur. J. Pharm. Biopharm. 87 (2) (2014) 227–235.
[19] M. Boegh, S.G. Baldursdottir, M.H. Nielsen, A. Müllertz, H.M. Nielsen, Development and rheological profiling of biosimilar mucus, Nord. Rheol. Soc. Annu Trans. 21 (2013) 233–240.
[20] V.L.N. Murty, J. Sarosiek, A. Slomiany, B.L. Slomiany, Effect of lipids and proteins on the viscosity of gastric mucus glycoprotein, Biochem. Biophys. Res. Commun. 121 (2) (1984) 521–529.
[21] C. Twarog, F. McCartney, S.M. Harrison, B. Illel, E. Fattal, et al., Comparison of the effects of the intestinal permeation enhancers, SNAC and sodium caprate (C(10)): isolated rat intestinal mucosae and sacs, Eur. J. Pharm. Sci. 158 (2021), 105685.
[22] L. Krupa, B. Bajka, R. Staroń, D. Dupont, H. Singh, et al., Comparing the permeability of human and porcine small intestinal mucus for particle transport studies, Sci. Rep. 10 (1) (2020) 20290.
[23] L.B. Knudsen, J. Lau, The discovery and development of liraglutide and semaglutide, Front. Endocrinol. 10 (2019) 155.
[24] R.M. Parlato, F. Greco, P.L. Maffettone, D. Larobina, Effect of pH on the viscoelastic properties of pig gastric mucus, J. Mech. Behav. Biomed. Mater. 98 (2019) 195–199.
[25] A. Curnutt, K. Smith, E. Darrow, K.B. Walters, Chemical and microstructural characterization of pH and [ca(2+)] dependent sol-gel transitions in mucin biopolymer, Sci. Rep. 10 (1) (2020) 8760.
[26] J.P. Celli, B.S. Turner, N.H. Afdhal, S. Keates, I. Ghiran, et al., Helicobacter pylori moves through mucus by reducing mucin viscoelasticity, PNAS. 106 (34) (2009) 14321.
[27] H.M. Yildiz, L. Speciner, C. Ozdemir, D.E. Cohen, R.L. Carrier, Food-associated stimuli enhance barrier properties of gastrointestinal mucus, Biomaterials. 54 (2015) 1–8.

[28] J. Seagrave, H.H. Albrecht, D.B. Hill, D.F. Rogers, G. Solomon, Effects of guaifenesin, N-acetylcysteine, and ambroxol on MUC5AC and mucociliary transport in primary differentiated human tracheal-bronchial cells, Respir. Res. 13 (1) (2012) 98.
[29] R. Balsamo, L. Lanata, C.G. Egan, Mucoactive drugs, Eur. Respir. Rev. 19 (116) (2010) 127–133.
[30] T.T. Kararli, Comparison of the gastrointestinal anatomy, physiology, and biochemistry of humans and commonly used laboratory animals, Biopharm. Drug Dispos. 16 (5) (1995) 351–380.
[31] A.C. Groo, F. Lagarce, Mucus models to evaluate nanomedicines for diffusion, Drug Discov. Today 19 (8) (2014) 1097–1108.
[32] J.Y. Lock, T.L. Carlson, R.L. Carrier, Mucus models to evaluate the diffusion of drugs and particles, Adv. Drug Deliv. Rev. 124 (2018) 34–49.
[33] D. Birch, R.G. Diedrichsen, P.C. Christophersen, H. Mu, H.M. Nielsen, Evaluation of drug permeation under fed state conditions using mucus-covered Caco-2 cell epithelium, Eur. J. Pharm. Sci. 118 (2018) 144–153.
[34] J. Thomsen, M.B. Sletfjerding, S.B. Jensen, S. Stella, B. Paul, et al., DeepFRET, a software for rapid and automated single-molecule FRET data classification using deep learning, eLife. 9 (2020), e60404.
[35] S.B. Jensen, S. Thodberg, S. Parween, M.E. Moses, C.C. Hansen, et al., Biased cytochrome P450-mediated metabolism via small-molecule ligands binding P450 oxidoreductase, Nat. Commun. 12 (1) (2021) 2260.
[36] F. Wan, S.S.R. Bohr, S.N. Kłodzińska, H. Jumaa, Z. Huang, et al., Ultrasmall TPGS–PLGA hybrid nanoparticles for site-specific delivery of antibiotics into Pseudomonas aeruginosa biofilms in lungs, ACS Appl. Mater. Interfaces 12 (1) (2020) 380–389.
[37] S.S.R. Bohr, P.M. Lund, A.S. Kallenbach, H. Pinholt, J. Thomsen, et al., Direct observation of Thermomyces lanuginosus lipase diffusional states by single particle tracking and their remodeling by mutations and inhibition, Sci. Rep. 9 (1) (2019) 16169.
[38] H.D. Pinholt, S.S.-R. Bohr, J.F. Iversen, W. Boomsma, N.S. Hatzakis, Single-particle diffusional fingerprinting: a machine-learning framework for quantitative analysis of heterogeneous diffusion, Proc. Natl. Acad. Sci. U. S. A. 118 (31) (2021) e2104624118.
[39] R.P. Thomsen, M.G. Malle, A.H. Okholm, S. Krishnan, S.S.R. Bohr, et al., A large size-selective DNA nanopore with sensing applications, Nat. Commun. 10 (1) (2019) 5655.
[40] M.E. Moses, P.M. Lund, S.S.R. Bohr, J.F. Iversen, J. Kæstel-Hansen, et al., Single-molecule study of thermomyces lanuginosus lipase in a detergency application system reveals diffusion pattern remodeling by surfactants and calcium, ACS Appl. Mater. Interfaces 13 (28) (2021) 33704–33712.
[41] S. Streck, S.S.R. Bohr, D. Birch, T. Rades, N.S. Hatzakis, et al., Interactions of cell-penetrating peptide-modified nanoparticles with cells evaluated using single particle tracking, ACS Appl. Bio. Mater. 4 (4) (2021) 3155–3165.
[42] B.C. Huck, O. Hartwig, A. Biehl, K. Schwarzkopf, C. Wagner, et al., Macro- and microrheological properties of mucus surrogates in comparison to native intestinal and pulmonary mucus, Biomacromolecules. 20 (9) (2019) 3504–3512.
[43] J. Ceulemans, A. Ludwig, Optimisation of carbomer viscous eye drops: an in vitro experimental design approach using rheological techniques, Eur. J. Pharm. Biopharm. 54 (1) (2002) 41–50.
[44] C. de Loubens, R.G. Lentle, R.J. Love, C. Hulls, P.W. Janssen, Fluid mechanical consequences of pendular activity, segmentation and pyloric outflow in the proximal duodenum of the rat and the guinea pig, J. R. Soc. Interface 10 (83) (2013) 20130027.
[45] M. Boegh, M. Garcia-Diaz, A. Mullertz, H.M. Nielsen, Steric and interactive barrier properties of intestinal mucus elucidated by particle diffusion and peptide permeation, Eur. J. Pharm. Biopharm. 95 (Pt A) (2015) 136–143.
[46] R. Shaikh, T.R. Raj Singh, M.J. Garland, A.D. Woolfson, R.F. Donnelly, Mucoadhesive drug delivery systems, J. Pharm. Bioallied Sci. 3 (1) (2011) 89–100.
[47] M.B. Stie, J.R. Gätke, F. Wan, I.S. Chronakis, J. Jacobsen, et al., Swelling of mucoadhesive electrospun chitosan/polyethylene oxide nanofibers facilitates adhesion to the sublingual mucosa, Carbohydr. Polym. 242 (2020), 116428.
[48] E.Y.T. Chen, N. Yang, P.M. Quinton, W. Chin, A new role for bicarbonate in mucus formation, Am. J. Phys. Lung Cell. Mol. Phys. 299 (4) (2010). L542-L9.
[49] I. d'Angelo, C. Conte, M.I. La Rotonda, A. Miro, F. Quaglia, et al., Improving the efficacy of inhaled drugs in cystic fibrosis: challenges and emerging drug delivery strategies, Adv. Drug Deliv. Rev. 75 (2014) 92–111.
[50] C.E. Wagner, B.S. Turner, M. Rubinstein, G.H. McKinley, K. Ribbeck, A rheological study of the association and dynamics of MUC5AC gels, Biomacromolecules. 18 (11) (2017) 3654–3664.
[51] O. Lieleg, I. Vladescu, K. Ribbeck, Characterization of particle translocation through mucin hydrogels, Biophys. J. 98 (9) (2010) 1782–1789.
[52] R.S. Crowther, C. Marriott, S.L. James, Cation induced changes in the rheological properties of purified mucus glycoprotein gels, Biorheology. 21 (1984) 253–263.
[53] J.M.H. Larsson, K.A. Thomsson, A.M. Rodríguez-Piñeiro, H. Karlsson, G. C. Hansson, Studies of mucus in mouse stomach, small intestine, and colon. III. Gastrointestinal Muc5ac and Muc2 mucin O-glycan patterns reveal a regiospecific distribution, Am. J. Physiol. Gastrointest. Liver Physiol. 305 (5) (2013). G357-G63.
[54] E.R. Vimr, K.A. Kalivoda, E.L. Deszo, S.M. Steenbergen, Diversity of microbial sialic acid metabolism, Microbiol. Mol. Biol. Rev. 68 (1) (2004) 132–153.
[55] M.P. Quintana-Hayashi, M. Padra, J.T. Padra, J. Benktander, S.K. Lindén, Mucus-pathogen interactions in the gastrointestinal tract of farmed animals, Microorganisms. 6 (2) (2018) 55.
[56] A.M. Sadowska, N-acetylcysteine mucolysis in the management of chronic obstructive pulmonary disease, Ther. Adv. Respir. Dis. 6 (3) (2012) 127–135.
[57] K.C. Kim, A. Hisatsune, D.J. Kim, T. Miyata, Pharmacology of airway goblet cell mucin release, J. Pharmacol. Sci. 92 (4) (2003) 301–307.
[58] P.C. Griffiths, P. Occhipinti, C. Morris, R.K. Heenan, S.M. King, et al., PGSE-NMR and SANS studies of the interaction of model polymer therapeutics with mucin, Biomacromolecules. 11 (1) (2010) 120–125.
[59] L. Sardelli, D.P. Pacheco, A. Ziccarelli, M. Tunesi, O. Caspani, et al., Towards bioinspired in vitro models of intestinal mucus, RSC Adv. 9 (28) (2019) 15887–15899.
[60] V. Barmpatsalou, I.R. Dubbelboer, A. Rodler, M. Jacobson, E. Karlsson, et al., Physiological properties, composition and structural profiling of porcine gastrointestinal mucus, Eur. J. Pharm. Biopharm. 169 (2021) 156–167.
[61] J.S. Mortensen, L. Saaby, S. Harloff-Helleberg, H.M. Nielsen, Barrier properties of ex vivo porcine intestinal mucus are highly independent of isolation and storage conditions, Eur. J. Pharm. Biopharm. 174 (2022) 106–110.
[62] S. Chu, M.L. Schubert, Gastric secretion, Curr. Opin. Gastroenterol. 28 (6) (2012) 587–593.
[63] L.J. Henze, N.J. Koehl, H. Bennett-Lenane, R. Holm, M. Grimm, et al., Characterization of gastrointestinal transit and luminal conditions in pigs using a telemetric motility capsule, Eur. J. Pharm. Sci. 156 (2021), 105627.
[64] S. Bhattacharjee, E. Mahon, S.M. Harrison, J. McGetrick, M. Muniyappa, et al., Nanoparticle passage through porcine jejunal mucus: microfluidics and rheology, Nanomedicine. 13 (3) (2017) 863–873.
[65] S. Fattah, M. Ismaiel, B. Murphy, A. Rulikowska, J.M. Frias, et al., Salcaprozate sodium (SNAC) enhances permeability of octreotide across isolated rat and human intestinal epithelial mucosae in Ussing chambers, Eur. J. Pharm. Sci. 154 (2020), 105509.
[66] N.N. Sanders, S.C. De Smedt, E. Van Rompaey, P. Simoens, F. De Baets, et al., Cystic fibrosis sputum: a barrier to the transport of nanospheres, Am. J. Respir. Crit. Care Med. 162 (5) (2000) 1905–1911.